

**SIGNIFICANCE OF ACTIVATION ENERGY IN PROCESS
METALLURGY**

THESIS SUBMITTED TO
NATIONAL INSTITUTE OF TECHNOLOGY,
ROURKELA
FOR THE AWARD OF THE DEGREE
OF
MASTER OF TECHNOLOGY
IN
METALLURGICAL AND MATERIAL ENGINEERING
BY

SANJAY RAJ
Roll No.: 211MM1366



DEPARTMENT OF METALLURGICAL AND MATERIALS
ENGINEERING,
NATIONAL INSTITUTE OF TECHNOLOGY, ROURKELA

May-2013

SIGNIFICANCE OF ACTIVATION ENERGY IN PROCESS METALLURGY

THESIS SUBMITTED TO
NATIONAL INSTITUTE OF TECHNOLOGY,
ROURKELA
FOR THE AWARD OF THE DEGREE
OF
MASTER OF TECHNOLOGY
IN
METALLURGICAL AND MATERIAL ENGINEERING
BY
SANJAY RAJ
Roll No.: 211MM1366

Under the supervision of

Prof. U.K.Mohanty
&
Prof. S.K.Sahoo



DEPARTMENT OF METALLURGICAL AND MATERIALS
ENGINEERING
NATIONAL INSTITUTE OF TECHNOLOGY, ROURKELA
May-2013



DEPARTMENT OF METALLURGICAL AND MATERIALS
ENGINEERING
NATIONAL INSTITUTE OF TECHNOLOGY, ROURKELA
ORISSA, INDIA - 769008

CERTIFICATE

This is to certify that the thesis entitled “**SIGNIFICANCE OF ACTIVATION ENERGY IN PROCESS METALLURGY**”, submitted to the National Institute of Technology, Rourkela by **Mr. SANJAY RAJ**, Roll No. **211MM1366** for the award of Master of Technology in Metallurgical and Materials Engineering, at the National Institute of Technology, Rourkela, is an authentic work carried out by him under supervision and guidance. The experimental work and analysis of results are original work of the student and have not been presented anywhere for the award of a degree to the best of our knowledge.

Prof. U.K. Mohanty

Department of Metallurgical and
Materials Engineering
National institute of technology
Rourkela – 769008

Prof. S.k.sahoo

Department of Metallurgical and
Material Engineering
National Institute of Technology
Rourkela – 769008

ACKNOWLEDGEMENT

It is an honour for us to present this project which has helped us in enhancing our practical and theoretical skills in various metallurgical aspects. We wish to Express our deep sense of gratitude to *Prof. B.C.Ray*, HOD, Metallurgical and Materials Engineering NIT Rourkela for giving us an opportunity to work on this project.

I am highly indebted to my guide *Prof. U.K .Mohanty, Prof. S.k.sahoo*, for his Consistent encouragement, guidance and support to carry out and complete this Project,

I would be highly obliged to extend our thanks to *Mr. Uday Kumar Sahu* for his immense support and help rendered while carrying out our experiments, Without which the completion of this project would have been at stake.

I would like to express my sincere gratitude to all the *faculty members and staff* of the department for their unflinching support, inspiration, and cooperation and providing me with all sort of official facilities in various ways for the completion of the thesis work.

I would also like to thank all my friends & my seniors, for extending their technical and personal support and making my stay pleasant and enjoyable.

At last but not the least; I remain really indebted to my family, *my parents* instilled strength especially at times when life was tough and supported me Throughout my difficulty period with endurance, with much love, I would like to thank *my younger brothers and sister* and who with their kind and encouraging words provided me with strong moral support.

Sanjay raj (211mm1366)
National Institute of Technology
Rourkela

Date: 2013-05-22

CONTENTS

	Page No.
Abstract.....	I
List of Figure.....	II
List of Tables.....	III
<u>Chapter-1</u>	
Introduction.....	1
1.1 Introduction.....	2-3
1.2 Objective.....	3
<u>Chapter-2</u>	
Literature Survey.....	4
2.1 Introduction of blast furnace.....	5-7
2.2 Blast Furnace Operation.....	7
2.2.1. Reactions in the Upper Zone.....	8
2.2.2. Reactions in the Middle Zone.....	8
2.2.3. Reactions in the Lower Zone.....	9
2.3 Blast Furnace Slag.....	10
2.3.1. General Overview.....	10
2.3.2. Forming methods of Slag.....	11-12
2.3.3. Slag Composition.....	12-13
2.3.4. Slag Viscosity.....	14
2.3.5. Calculation of viscosity.....	15
2.3.6. Flow Characteristics of slag.....	15
2.4.0 Activation Energy.....	16
2.4.1 Activation energy of blast furnace slag.....	16-17
2.4.2 Factor affecting of activation energy.....	17-18
2.4.3 Methods of estimation of activation energy...	18-22
2.4.4 Available Literature on Estimation of Activation Energy-22, 23	

Chapter-3

EXPERIMENTAL.....	25
3.1. Sample Preparation.....	26
3.2. Experimental Apparatus.....	27-30
3.2.1. Planetary Ball Mill.....	27
3.2.2. TG-DSC.....	28
3.2.3. High temperature viscometer.....	28
3.2.4. High Temperature Microscope.....	29
3.2.5. XRD Phase Analysis.....	30
3.2.6. SEM Analysis.....	30
3.3. Experimental Procedure.....	31-35

Chapter-4

RESULTS AND DISCUSSION.....	36
4.1 RESULT.....	37
4.1.1 Activation energy calculation.....	37-43
4.1.2 Viscosities Measurements.....	43-44
4.1.3 XRD Analysis.....	44
4.1.4 Flow characterisation of blast furnace slag.....	45
4.1.5 Microstructure Analysis by SEM.....	46
4.2 DISCUSSION.....	47

Chapter-5

CONCLUSION.....	48
5. Conclusion.....	49
FUTURE SCOPE.....	49
REFERENCES.....	50-52

Abstract

A study of thermal behaviour, thermal degradation kinetics, and effect of composition on flow characterisation of blast furnace slag is important to Understanding the flow characteristics of blast furnace (B/F) slag. It is an important parameter for efficiency/productivity of a blast furnace. In the present study flow characteristics of five different B/F slag (C/S: 1.04, 1.192, 1.107, 1.101, and 1.189) were investigated. This study was predominantly based on the estimation of activation energy. The activation energy was estimated using two methods: differential scanning calorimetry (DSC) and High temperature viscometer. DSC of different slag were measured at 30-1300°C @ 2°, 4°, 6°, 8° and 10°C/min. Activation energy was estimated from such DSC plots using Kissinger and Ozawa methods. It was observed that activation energy is largely dependent on C/S ratio of B/F Slag – The activation energy decreases with increase in C/S ratio. The flow characteristics of different B/F slag were also investigated by high temperature heating microscope, X-ray diffraction (XRD) and scanning electron microscope (SEM). The estimated IDT (initial deformation temperature), ST (softening temperature), HT (hemispherical temperature) and FT (fusion temperature) of different B/F slag was shown in table. Phase analysis of XRD and SEM micrographs support the results of flow characteristics measured by heating microscope.

Keywords: Activation Energy, DSC, Viscosity, B/F slag, heating rate, XRD.

List of Figures

Figure no 2.1: Schematic diagram showing Blast Furnace Process.

Figure no 2.2: Schematic sectional diagram of the internal zones in a blast furnace.

Figure no 3.1: Coning and Quartering.

Figure no. 3.2: A four station Planetary Ball Mill

Figure no.3.3: Simultaneous Thermo Analysis (TG-DSC or TG-DTA) in wide temperature range

Figure no.3.4: VIS 403 Rotating High Temperature Viscometer.

Figure no 3.5: Pictorial view of Leitz heating microscope.

Figure no 3.6: X-ray Diffraction Machine

Figure no.3.7: Scanning electron microscopic Machine (SEM).

Figure no. 4.1: DSC curves of powdered slag samples (a), (b), (c), and (d).

Figure no 4.2: Activation Energy vs. C/S ratio plot.

Figure no 4.3: Plot between Activation Energy vs. MgO%

Figure No-4.4. Viscosity vs. Temperature graph.

Figure no 4.5: .XRD pattern of slag sample.

Figure no 4.6- flow characteristic image of sample observed through Leitz Heating Microscope

Figure 4.7 (a) SEM micrographs *at 500 magnifications* of powder sample, (b) SEM micrographs at 500 magnification of sample no 1 whose C/S ratio is 1.192.

LIST OF TABLES

Table 2.1: Chemical Composition of Industrial Blast Furnace Slag.

Table 2.2: Comparative values of viscosity of some liquids

Table 3.1: Chemical composition (wt. %) of different blast furnace slag

Table 4.1: Peak temperature of different obtained from DSC curve.

Table 4.2: Different DSC analysis plots by (a) Kissinger (b) Ozawa methods for the blast furnace slag studied

Table 4.3. Tabulation of Activation Energy by different methods and C/s ratio

Table 4.4: Tabulation of Activation Energy and MgO% by different methods

Chapter-1

INTRODUCTION

1. INTRODUCTION

The iron and steel slag that is generated as a by-product of iron and steel manufacturing processes can be broadly categorized into blast furnace slag and steelmaking slag. Iron and steel slag refers to the metal manufacturing slag [1,2] that is generated during the process of manufacturing iron and steel products.

Literature study reveals blast furnace slag which is recovered by melting separation from blast furnaces [3] that produce molten pig iron. It consists of non-ferrous components, contained in the iron ore together with limestone as an auxiliary materials and ash from coke (CaO , SiO_2 , MgO , Al_2O_3 , TiO_2 , FeO , K_2O ,). Approximately 290 kg of slag is generated for each ton of pig iron. When it is rejected from blast furnace, the slag is in molten at a temperature of approximately $1,500^\circ\text{C}$. Depending on the cooling method used, it is classified either as air-cooled slag or granulated slag.

During iron making the blast furnace is a complex high temperature counter current reactor in which iron bearing materials (ore, sinter/pellet) and coke are alternately charged along with a suitable flux to create a layered burden in the furnace. The iron bearing material layers start softening and melting in the cohesive zone under the influence of the fluxing agents at the prevailing temperature which greatly reduces the layer permeability that regulates the flow of materials (gas/solid) in the furnace. It is the zone [1] in the furnace bound by softening of the iron bearing materials at the top and melting and flowing of the same at the bottom. A high softening temperature coupled with a relatively low flow temperature would form a narrow cohesive zone lower down the furnace. This would decrease the distance travelled by the liquid in the furnace there by decreasing the Silicon pick-up. On the other hand the final slag that trickles down the Bosh region to the Hearth in the furnace should be a short slag that starts flowing as soon as it softens. Thus activation energy [4, 5] behaviour of blast furnace slag is important parameter to evaluate the flow characteristics of slag.

Activation Energy detects the stability of main constituents. A lower value of that energy (constituents' energy) put the relative value of Activation Energy. Activation energy gives an idea about the optimum reaction conditions in process chemistry, it gives an idea about thermal stability and the expected lifetime of a slag to be kept at a certain temperature or it provides information in quality research. The activation energy of the thermal decomposition [6] reaction of the relative bond strengths within the molecules studied.

Keeping the above in mind, to obtain objective of this experiment we collected Blast furnace slag from Rourkela steel plant contained at different heat (over a time period) and then determined the chemical composition of slag. In addition to employing three different experimental methods used to determine the activation energy of blast furnace slag.

Firstly used generalised Kissinger and Ozawa equation [7], which is derived from Arrhenius Equation, apply a range of approximations for the temperature integral. In which a simplified assumption that the transformation rate during a reaction is the product of two functions, one depending solely on the temperature, T , and the other depending solely on the fraction transformed \dot{q} . It calculated with the help of DSC measurements instruments at slow heating rates (2, 4, 6, 8, 10⁰C/min.). Other than this methods Ozawa [8] method applied to analytical study of Activation Energy of slag. And also plotting the graph between Activation Energy vs. C/S ratio and also vs. MgO % this gives idea about variation of Activation Energy with these values Second phase of the experiment involve calculation of activation energy of slag by viscosity meter machine which depends upon the viscous property of the slag. Viscosity of slag increases by the presence of silica and alumina whereas the presence of calcium oxide reduces the viscosity which is function of temperature of melt [9].

Next work in this project is to analyse crystallization behaviour of diffused slag of different chemical composition. It related with Activation Energy of slag. We therefore tested by several determination techniques XRD for phase analysis, SEM for morphological study, High Temperature Heating Microscope to determine flow temperature of slag .the quality or consistency of a slag and identified the unknown materials in slag.

1.2 Objective

Objective of this work is to measure the activation energy of the blast furnace slag, collected from different sources with varied chemical composition and to correlate the activation energy with the chemical composition of the slag. This would provide a basis of understanding the variation of activation energy of the slag. Objectives of this thesis are -

1. Determination of Activation energy of blast furnace slag by two techniques.
 - A. TG-DSC.
 - B. Viscosity measurements by High Temperature Viscometer.
2. Phase Analysis by X-ray Diffraction Techniques (XRD) to understand the variation in activation energy.

Chapter-2

LITERATURE SURVEY

2.1 Introduction of Blast Furnace

A blast furnace is a type of metallurgical furnace used for smelting to produce industrial metals, generally iron. The blast furnace is fundamentally a vertical steel shaft or stack varying in height from 24 to 33 meters with a diameter at the hearth of about 8.5 meters. Generally the total volume for production of pig iron is more than 1400 cubic meters. And steel structural cylinder is lined with hard-fired alumina refractory brick to a depth of approximately 1.2 meters. The total weight of the furnace is approximately 9000 metric tons. The blast furnace has charging arrangements at the top and a means of running off the pig iron and slag at the bottom.

Element of blast furnace construction- the main unit consists of

- (1) The hearth (Lower section),
- (2) The bosh (Middle section),
- (3) The stack and charging mechanism (Upper section).

The purpose of a blast furnace is to chemically reduce and physically convert iron oxides into liquid iron called "hot metal". The blast furnace is a huge, steel stack lined with refractory brick, where iron ore, coke and limestone are dumped into the top, and preheated air is blown into the bottom. The raw materials require 6 to 8 hours to descend to the bottom of the furnace where they become the final product of liquid slag and liquid iron. These liquid products are drained from the furnace at regular intervals. The hot air that was blown into the bottom of the furnace ascends to the top in 6 to 8 seconds after going through numerous chemical reactions [3]. Once a blast furnace is started it will continuously run for four to ten years with only short stops to perform planned maintenance.

The sources of iron are its ores in which iron is contained mainly as its oxides such as hematite (Fe_2O_3) or magnetite (Fe_3O_4) and sometimes in small proportions as hydroxides and carbonates. Hematite constitutes the largest portion of all the ores used for blast furnace iron making. When pure, hematite contains about 70% and magnetite about 72.4% of iron. But in actuality, the iron content of the ores ranges from 50-65% for rich ores and 30-50% for lean ores and the remainder is gangue which consists mostly of silica and alumina as well as minor amounts of moisture and chemically- combined water.

Iron Ore processing for the Blast- Before introducing the blast furnace reaction it is important to know the Iron Ore Processing for the Blast Furnace. It is based on flowing steps

Mining Iron Ore – Ores have been produced subsequently wherever erosion exposed suitable structures to the particular conditions of climate, topography, tectonic stability required for the long process. Mining iron ore begins at ground level. Taconite is identified by diamond drilling core samples on a grid hundreds of feet into the earth. Taconite rock comprises about 28 percent iron; the rest is sand or silica. These samples are analyzed and categorized so that mining engineers can accurately develop a mine plan.

Crushing the Ore - The crude taconite is delivered to large gyrator crushers, where chunks as large as five feet are reduced to six inches or less. More than 6,000 tons of taconite can be crushed in one hour. The crushed material is transferred by belt to an ore storage building, which holds up to 220,000 tons of taconite. An apron feeder sends the ore to the concentrator building for grinding, separating, and concentrating.

Concentrating - The crude taconite is now roughly the size of a football or smaller. A series of conveyor belts continuously feed the ore into the large 27-foot-diameters, semi-autogenously primary grinding mills. Water is added at this point to transport it (94 percent of the water is recycled, while the rest is lost through evaporation). The product is called “filter cake”, and is now ready for mixing with the Binding agent. Once the filter cake is complete; it is deposited into a surge bin. It then travels onto a feeder belt and from there to a conveyor where betonies, a bonding agent, are added. Betonies are clay from Wyoming used to help iron ore concentrate stick together when rolled into pellets. About 16 pounds of Betonies are added to every ton of iron ore concentrate. Small amounts of limestone (1%) are also added and mixed with the concentrate at this point. Limestone is added to meet the requirements of steel customers in the blast furnace process.

Palletizing - A pellet plant contains a series of balling drums where the iron ore concentrate is formed into soft pellets, in much the same manner that one rolls a snowball, to make a pellet about the size of a marble (between 1/4" and 1/2"). Pellets are screened to meet the size specification, with undersized or oversized pellets crushed and returned to the balling drums.

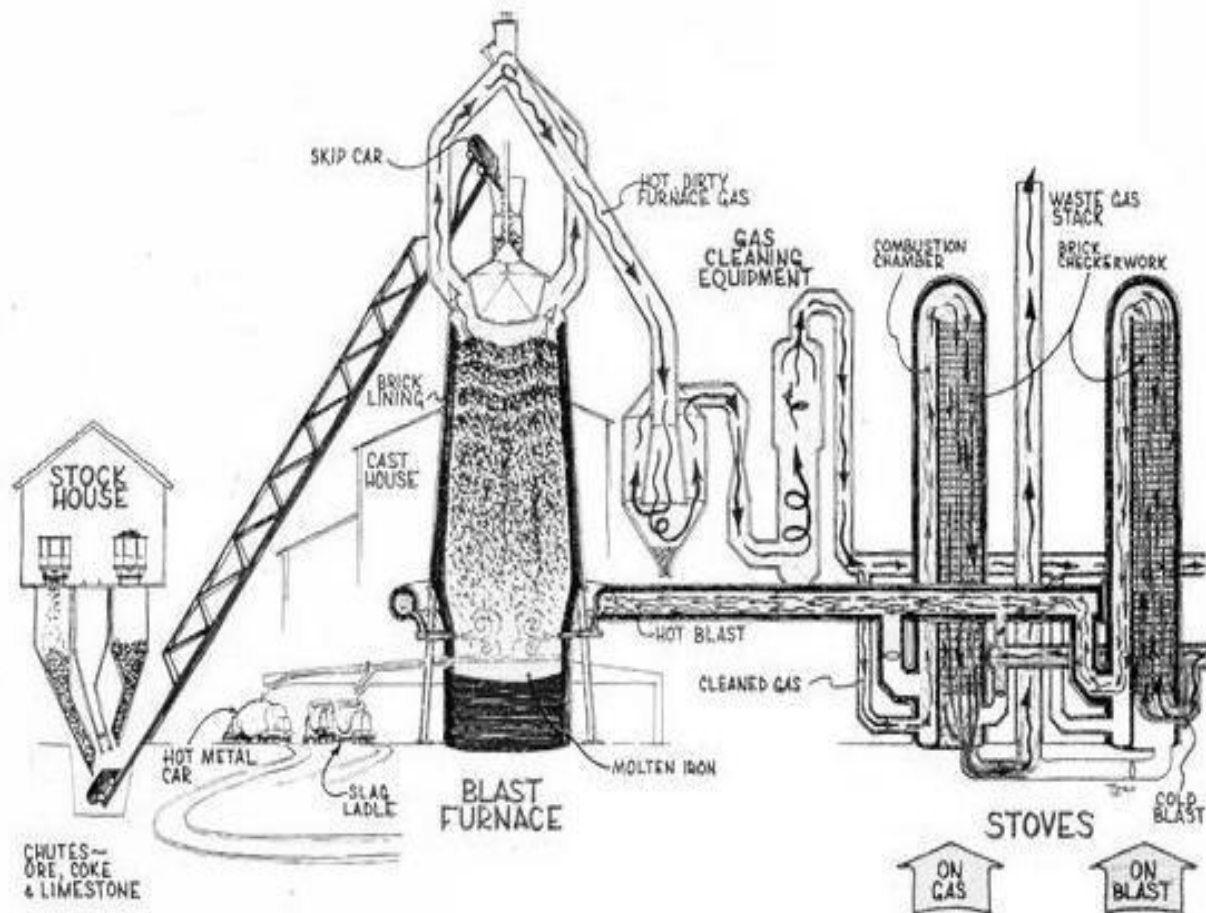


Figure 2.1: Schematic diagram showing Blast Furnace Process.

2.2 Blast Furnace Operation

In blast furnace operation, the charge components ore, flux, and coke are carried in successive layers and in carefully calculated proportions to the top of the furnace [3]. They are introduced into the furnace through the bell valves and the stack is loaded to a height 1.8 to 3 meters above the valve system. Air is preheated to about 1000°C in heaters attached to the furnace. It is then blown in through vents spaced around the furnace near its lower end, leaving enough space for the slag and molten iron to collect in the bottom below them. It is this blast of air that gives furnace its name.

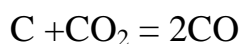
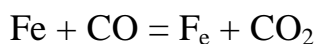
The blast furnace operates on a counter current principle; the charge moves slowly down in the furnace and current of gas that reacts with this charge moves upward. This operation is reduction smelting.

Blast furnace reaction gives three zone reactions [10].

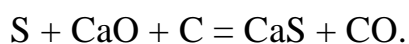
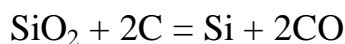
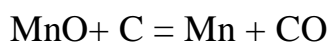
2.2.1 Reactions in the lower zone

In the Bosh area of the furnace where the burden starts to soften and melt, direct reduction of the iron [and other] oxides and carbonization by the coke occurs at 1,000-1,600 C. Molten iron and slag start to drip through to the bottom of the furnace. Between the bosh and the hearth are the tuyeres [water cooled copper nozzles] through which the blast combustion air, preheated to 900-1,300°C, often enriched with oxygen is blown into the furnace [3, 10].

Immediately in front of the tuyeres is the combustion zone, the hottest part of the furnace, 1,850-2,200 C, where coke reacts with the oxygen and steam in the blast to form carbon monoxide and hydrogen [as well as heat] and the iron and slag melt completely.



Lower zone [10] is higher temperature zone in which reduction of Si and Ti occurs while the oxides of Mg, Ca and Al are highly stable such that they are reduced to a negligible amount. At the high temperature the reduction of Mn from its monoxide takes place which is quite difficult and Cr and V behaves in similar manner as Mn.

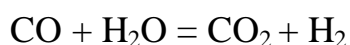


2.2.2 Reactions in the Middle Zone.

In the Middle part of the blast furnace, indirect reduction of the iron oxides (wustite) by carbon monoxide and hydrogen occurs take place at 700-1,000 C.

The ratio of CO/CO₂ gas is 2.3, a value exhibiting equilibrium with Fe-FeO (Eq.) The indirect reduction will be more if the height of this Zone (800-1000°C temperature zone) is large since the contact time is longer between gas/solid.

This zone may occupy 50-60% of the furnace volume. The extent of this zone is important because the Wustite should be given as much opportunity as possible for getting reduced indirectly. Another reaction of importance which occurs in the middle zone is the water-gas shift reaction:



2.2.3 Reactions in the Upper Zone.

In the upper or preheating zone of the furnace, free moisture is driven off from the burden materials and hydrates and carbonates are disassociated. The temperature of the gas ascending from the middle zone falls rapidly from 800-1000°C to 100-250°C and that of solids rises from ambient to 800°C in this zone Carbon deposition and Partial or complete reduction of hematite and magnetite to their lower oxides occurs

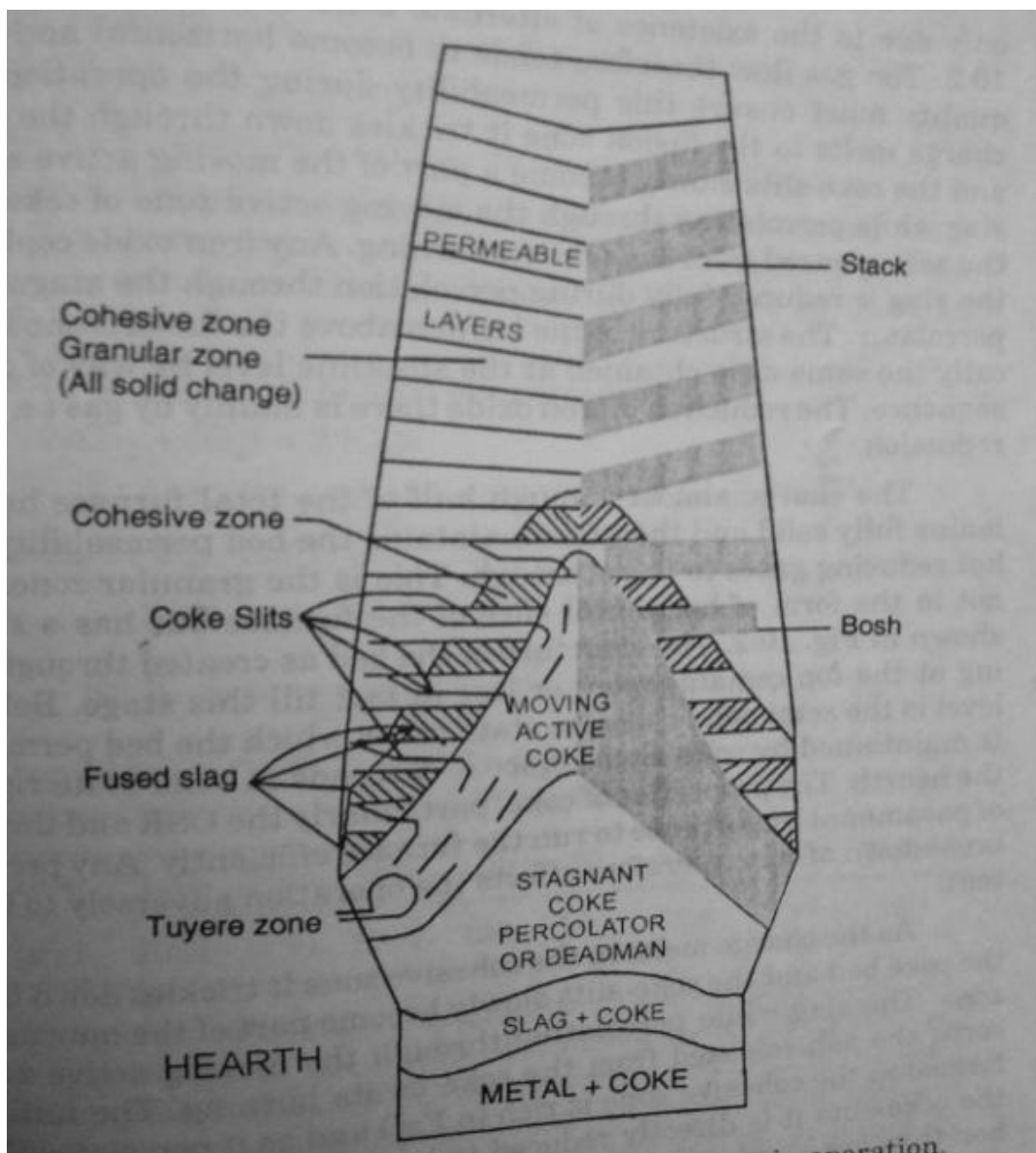
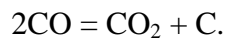


Figure 2.2: Schematic sectional diagram of the internal zones in a blast furnace.

2.3 Blast Furnace Slag

2.3.1. General Overview-

Blast furnace slag as “the non-metallic product consisting essentially of silicates and alumino silicates of calcium and other bases that is developed in a molten condition simultaneously with iron in a blast furnace ” Iron and steel slag refers to the type of metal manufacturing slag that is generated during the process of manufacturing iron and steel products. The term "slag" originally referred to slag produced by metal manufacturing processes, however it is now also used to describe slag that originates from Molten waste material when trash and other substances are disposed of at an incinerator facility.

In the production of iron, the blast furnace is charged with iron ore, flux stone (limestone and/or dolomite) and coke for fuel. Two products are obtained from the furnace: molten iron and slag. The slag consists primarily of the silica and alumina from the original iron ore, combined with calcium and magnesium oxides from the flux stone. It comes from the furnace in a molten state with temperatures exceeding 1480°C (2700°F).

It play important role as they protect the metal and remove undesirable impurities. Usually a liquid slag layer covers the molten metal and carries out the following functions [3].

- (i) It seals off the metal from oxygen and prevents oxidation
- (ii) It removes undesirable elements (e.g. S, P) from the metal
- (iii) It helps to remove non-metallic inclusions (e.g. by flotation etc)
- (iv) It reduces the heat losses from the metal surface and prevents the “*skull formation*” and
- (v) In the continuous casting of steel liquid slag infiltrates continuously between the metal and mould and it provides both lubrication and control of the heat extraction

2.3.2. Forming methods of Slag

There are four distinct methods [2, 3] of processing the molten slag. Which is air cooled, expanded, pelletized and granulated. Each of these methods produces a unique slag material. This is given below of this topic.

1. Air-Cooled slag (Atmospheric cooling)

Air-Cooled Blast Furnace (ACBF) Slag as defined in ASTM C 125 [2] is: “The material resulting from solidification of molten blast-furnace slag under atmospheric conditions. Subsequent cooling may be accelerated by application of water to the solidified surface.” The solidified slag characteristically has a vesicular structure with many non-connected cells. ACBF slag crushes to angular, roughly cubical pieces with a minimum of flat or elongated fragments. The rough vesicular texture of slag gives it a greater surface area than smoother aggregates of equal volume and provides an excellent bond with Portland cement and high stability in bituminous mixtures.

2. Expanded slag (Controlled water cooling)

Controlled quantities of water are used to accelerate the solidification process of molten blast furnace slag, resulting in a low density material. The solidified expanded slag is crushed and screened for use as a lightweight structural aggregate. It is angular and cubical in shape, with negligible flat or elongated particles. Due to the action of the water and resulting steam on the solidification process, the open cellular structure of the particles is even more pronounced than particles of air cooled blast furnace slag.

3. Pelletized (Accelerated cooling)

In the pelletizing process, a molten blast furnace slag stream is directed onto an inclined vibrating feed plate where it is quenched with water. The addition of water at this stage causes the slag to foam. While in this expanded pyroplastic state the slag stream flows from the feed plate onto a revolving finned drum. As the drum rotates, the fins repeatedly strike the slag stream with sufficient force to propel the slag into the air, dispersing it and forming spherical droplets. These droplets, or slag pellets, freeze rapidly to a solid state as they are launched through the air away from the pelletizer. It has a unique internal cellular structure within each slag pellet. This cellular structure (many voids only detectable with the aid of an electron microscope) is contained within a smooth spherical skin. The combination of these

characteristics leads to the formation of a low density aggregate, with diverse applications as a construction material [3].

4. Granulated (Water quenching)

The most common process for granulating blast furnace slag involves the use of high water volume, high pressure water jets in direct contact with the molten blast furnace slag at a ratio of approximately 10 to 1 by mass. The molten blast furnace slag is quenched almost immediately, forming a material generally smaller than a #4 sieve.

2.3.3. Slag Composition

The principle constituents of blast furnace slag are silica, alumina, calcium and magnesia which comprise 95% of slag's total makeup. Minor elements include manganese, iron and sulphur compounds as well as trace quantities of several others. Analysis of most blast furnace slags falls within the ranges that are shown below. The major oxides do not occur in free form in the slag. In air-cooled BF slag, they are combined to form various silicate and aluminosilicate minerals such as melilite, merwinite, wollastonite, etc., as found in natural geological forms. In the case of granulated and pelletized slag, these elements exist primarily as glass. The chemical composition [11] of slag from a given source varies within relatively narrow limits since raw materials charged into the furnace are carefully selected and blended

The major constituents of the slag include the following,

Major elements are:		Minor elements are:	
➤ SiO ₂	– 32-42% ,	S	– 1-2%
➤ Al ₂ O ₃	– 7-16% ,	FeO	– 1-1.5%
➤ CaO	– 32-45% ,	MnO	– 0.2-1.0%
➤ MgO	– 5-15% ,	TiO ₂	– 1.01%
		K ₂ O+Na ₂ O	– 1%
		Trace Oxides	– 0.5%

In this project work I have taken 5 sample of blast furnace slag in which slag constituents are.

Sample	SiO ₂	Al ₂ O ₃	CaO	MgO	TiO ₂	Na ₂ O	K ₂ O	Fe ₂ O ₃	C/S
1	31.86	16.92	38	10.23	0.7	0.98	0.48	0.66	1.192
2	33.25	16.31	36.84	10.56	0.82	1.1	0.52	0.54	1.107
3	32.48	17	35.78	11.88	0.55	1.1	0.52	0.6	1.101
4	31.08	17.04	36.96	11.22	0.5	1.8	0.88	0.40	1.189
5	34.32	16.58	36.2	9.57	0.55	1.36	0.82	0.53	1.054

Table2.1. Chemical Composition of Industrial Blast Furnace Slag

2.3.4. Slag Viscosity

Viscosity involves transporting one layer of liquids over another layer i.e. flow phenomena. In the study of blast furnace slag various important phenomena occurs such as the heat transfer, mass transfer and the chemical reactions between the slag and metal. And it depends on the flow phenomena of the slag hence study of viscosity is important [12]. Slag viscosity also determines the slag-metal separation efficiency, and subsequently the metal yield and impurity removal capacity.

In blast furnace iron making process, slag viscosity is a very important physical property, because it influences the furnace operation in many ways. The viscosity of the slag affects the degree of desulphurization, coke consumption, smoothness of operation, gas permeability, heat transfer etc.

The blast furnace slag behaves as a Newtonian fluid due to the presence of shear stresses applicable on the slag [13, 14]. This shear stress is the iconic and molecular structure that governs the viscosity of the blast furnace slag. Viscosity of a slag is strongly influenced by the chemical composition, structure and the temperature. Thus, for smooth furnace operation, it is always advisable to have a low viscosity slag which helps in smooth transport of ions from the slag and metal interface to the liquid slag [15].

The calculation of viscosity by Arrhenius equation [16] mainly depends on temperature and chemical composition.

$$\dot{\eta} = A \cdot \exp(E/RT).$$

Where η is called the **kinematic viscosity** of slag and has the dimensions of $L^2 t^{-1}$. The kinematic viscosity is also referred to as the **momentum diffusivity** of the fluid, i.e. the ability of the fluid to transport momentum. In the metric system, the unit of viscosity is the Poise ($1P=1 \text{ g cm}^{-1} \text{ s}^{-1}$), which is subdivided to 100 centipoise (cP). And $A = Pre$ – exponential term. E = Activation energy for viscous flow. R = Gas constant. T =Temperature, in absolute scale.

Slag viscosity is a transport property that relates to the reaction kinetics and the degree of reduction of the final slag. The viscosity of the slag controls the aerodynamics such as the gas permeability and the heat transfer this in turn affects the efficiency of the blast furnace.

The viscosity of the blast furnace slag governs the reaction rates in the furnace by its effect on the diffusion of ions through the liquid slag to and from the slag metal interface.

A process of depolymerisation lowers the viscosity of the slag. An increase in basicity decreases the viscosity of the blast furnace slag breaking the three dimensional silicate network in to discrete anionic groups thereby causing depolymerisation.

The component of slag namely silica and alumina increase the viscosity whereas the presence of calcium oxide reduces the viscosity. The melting zone of slag determines the cohesive zone of blast furnace and hence the fluidity and melting characteristics of slag play a major role in determining the blast furnace productivity.

Fluid	Temperature ($^{\circ}\text{C}$)	Viscosity ($\text{Kgs}^{-1}\text{m}^{-1}$)	Density (Kgm^{-3})
Molten iron	1550,	6.70×10^{-3}	7.21×10^3
	1600	6.10×10^{-3}	7.16×10^3
High-iron slag	1200	3.50×10^{-1}	4.50×10^3
Low-iron slag	1500	5.00×10^{-1}	3.50×10^3

Table 2.2 Comparative standard values of viscosity of some liquids

2.3.5: Calculation of viscosity

In our experimental work calculation of viscosity of blast furnace slag is done by VIS 403 Rotating High Temperature Viscometer which has viscosity range 10^1 - 10^8 dPas, Max Temperature 1700°C, crucible material-PtAu5%, max speed-800 rpm, Torque range 0-150mNm, and Atmosphere -air or inert gas, purge gas.

2.3.6: Flow Characteristics of Blast Furnace Slag

High temperature microscope is used to determine flow characteristics of slag sample. It has got four characteristics temperatures to be studied:

- **Initial deformation temperature (IDT)** - Initial deformation temperature is the temperature at which the first rounding up of the edges of the cube-shaped sample specimen takes place. In fact this is the temperature at which the first sign of the change in shape appears. Rheologically this temperature symbolizes the surface stickiness of the slag.
- **Softening Temperature (ST):-** It is the temperature at which the outline of the shape of the sample starts changing and is reported as the temperature at which the sample shrinks by one division or the temperature at which the distortion of the sample starts. Rheologically this temp symbolizes the start of plastic distortion.
- **Hemispherical Temperature (HT):-** It is the temperature at which the sample has fused down to hemispherical shape and is measured as the temp at which the height of the sample is equal to the half of its base length. This is defined as the fusion point or the melting point in German Industrial Standards 51730 [10]. Rheologically this temperature symbolizes the sluggish flow of the slag.
- **Flow Temperature (FT):-** It is the temperature at which the sample liquefies and is reported as the temperature at which the height of the sample is equal to one-third of the height that it had at HT (hemispherical temperature). Rheologically this temperature symbolizes the liquid mobility of the slag.

2.4.0 Activation energy and its importance

In reaction point of view Activation energy is a term introduced in 1889 by the Swedish scientist Svante Arrhenius that is defined as the minimum energy that must be input to a chemical system, containing potential reactants, in order for a chemical reaction to occur.

Activation energy may also be defined as the minimum energy required starting a chemical reaction. The activation energy of a reaction is usually denoted by E_a and given in units of kilojoules per mole.

The Arrhenius equation gives the quantitative basis of the relationship between the activation energy [4] and the rate at which a reaction proceeds. From the Arrhenius equation, the activation energy can be expressed as

$$k = Ae^{-E_a/RT}$$

Where A is the frequency factor for the reaction, R is the universal gas constant, T is the temperature (in Kelvin), and K is the reaction rate coefficient [17].

In metallurgical point of view the activation energy give the idea about thermal decomposition reaction of the relative bond strengths within the molecules studied.

The additional energy required to break the bond and to start the reaction is also called activation energy.

In another point of view the content E , called activation energy, is often interpreted as the energy barrier opposing the reaction.

2.4.1: Activation energy of blast furnace slag

Slag is the by-product of steel making process in which the component of the pig iron and steel-scrap are modified in order to produce steel.

During production of pig iron it should be important to know the idea about the activation energy of blast furnace slag in following point of view.

- It play important role in adhesion of ash particles to the walls of a reactor,
- It give an idea about solidification of slag,
- Slag and metal separation temperature and time calculation,

- Calculation of heat content change of slag,
- Representation of endothermic and exothermic reaction [18].
- It gives the idea about recrystallization temperature [18].
- Energy barrier of slag flowing properties,
- Movement of flow units involves breaking of Si-O bonds (Heat of dissociation) [19].
- Time taken to the reaction of slag formation [17].
- Viscosity property of slag [20].
- The energy required to move one layer of silicate group with respect to the other layer .i.e. the number of ionic bonds which have to be broken or distorted in order to enable the group to move,
- It gives the melting point of slag [21].
- It gives the idea about nucleation and grain growth [22].

2.4.2: Factor affecting the activation energy

Activation energy of blast furnace slag affected by

- **Temperature** - At the high temperature region of furnace, slag initially has highly active i.e. have more energy of slag practical means have less activation energy ,similarly those practical which has less temperature has more activation energy. This is due to the Increase in speed of particles do there are more successful collisions with particles having the required activation energy.
- **Concentration and pressure** - If the concentration or pressure of a slag is high, there will be more particles within a given space and therefore collision of particle more, so the rate of reaction also increases which give flow characteristics of slag is high means activation energy become less.
- **Physical state** - for the calculation of activation energy of slag, particle size must be in power shape because if one of the slag particles is in large shape then the reaction can only take place on the surface of the solid which will not give correct result in calculation of activation energy of slag. The smaller the size of the slag particles, the greater the area that the reaction can take place is high.
- **Composition of the slag.** Within the range of compositions study, the net-work breaking ability of Mg, Al, Ca, Si oxides are different which give the different activation energy.

- **Percentage of CaO** - Those slag sample which has more percentage of CaO is more basicity [21] so it also increase the liquidus temperature (T_{liq})[4] of the slag and thereby reduce the amount of liquid slag formation which result in high activation energy of slag.
- **Structure of melted slag** - Since thermodynamics gives a description of bond strength which is related with activation energy of slag.
- **Basicity of slag** - Some slag have a highly basicity ($CaO/SiO_2 > 2$) and consequently the Si^{4+} ions are predominantly in the form of monomers. Which give the high activation energy of slag [2].
- **Surface tension** – These properties predominantly depend upon surface and not on the bulk, in mixtures, the constituents with the lowest surface tension (slag contain B_2O_3) will tend to occupy the surface layer. When there are more than two surface-active components in the slag (CaF_2 and B_2O_3) there will be competition for the surface sites which alter the activation energy of slag.

2.4.3: Numerical Methods of Estimation of Activation Energy

A general objective of the analysis and prediction of thermally activate reactions is the derivation of a complete description of the progress of a reaction that is valid for any thermal treatment as a [23, 24]

- Isothermal by linear heating and
- Non-isothermal treatment

Many researchers make the simplifying assumption that the transformation rate during a reaction is the product of two functions, one depending solely on the temperature T , and the other depending solely on the fraction transformed, α

$$\frac{d\alpha}{dt} = f(\alpha)k(t) \quad (1)$$

Temperature dependent function follows **Arrhenius** type dependency,

$$K_T = k_0 \exp(-E/RT) \quad (2)$$

The quantity α is the degree of conversion, $f(\alpha)$ is a mathematical function whose form depends on the reaction types and K_T is the temperature dependent rate constant, K_0 is pre exponential factor, E is the activation energy and R is the gas constant, 8.314 J/mol K.

From (1) and (2) this give basic equation is,

$$\frac{d\alpha}{dt} = Kf(\alpha)\exp - E/(RT) \quad (3)$$

For isothermal conversion:

It has been known that for analysis linear heating experiment (heating at constant rate), highly accurate and reliable activation energy analysis methods [25] can be obtained by applying accurate approximations of the temperature integral so from equation no. (3) Is integrated by separation of variables.

$$\int_{t_0}^{t_f} \frac{d\alpha}{f(\alpha)} = \frac{K}{\beta} \int_{t_0}^{t_f} \exp(-E/RT) dt = \frac{K_0}{\beta} \left[\int_0^{t_f} \exp\left(\frac{-E}{RT}\right) dt - \int_0^{t_0} \exp\left(\frac{-E}{RT}\right) dt \right] \quad (4)$$

Where T_f is the temperature at an equivalent (fixed) state of transformation, to be the start temperature of the linear heating experiment, and β is the heating rate. The integrals on the right hand side are generally termed temperature integrals (or 'Arrhenius integral'). We can write Eq. 4 as:

$$\int_{t_0}^{t_f} d\alpha/f(\alpha) = \frac{K_0}{\beta} [I(T_f) - I(T_0)] \quad (5)$$

Where $I(T_0)$, $I(T_f)$ are the temperature integrals on the right hand side of Eq. 4. The derivation proceeds by noting that of the last two terms, one is much smaller than the other

$$\int_0^{t_0} \exp\left(\frac{-E}{RT}\right) dt \ll \int_0^{t_f} \exp(-E/RT) dt$$

And hence $I(T_0)$, the smaller term in above equation (5) so we can neglect

Thus it follows that,

$$\int_{t_0}^{t_f} \frac{d\alpha}{f(\alpha)} \cong \frac{K}{\beta} \int_{t_0}^{t_f} \exp(-E/RT) dt \quad (6)$$

Through applying a suitable approximation for the temperature integral on the right of the latter equation a range of well-known and lesser known isoconversion methods for activation energy analysis can be derived [25]. These methods include the Kissinger method [26], the Kissinger–Akahira–Sunose (KAS) method [21, 27] (also termed the generalised Kissinger method), All of these methods involve the plotting of $1/T_f$ vs. a logarithmic function which depends on the heating rate and often the temperature and all of these methods neglect the last integral term in Eq. 4 ($I(T_0)$ in Eq. 5).

The general equation is:

$$\ln \frac{\beta}{(Tf)^k} = -A \frac{E}{RTf} + C \quad (7)$$

Where k is a constant depending on the approximation of the temperature integral employed [28], and A and C are constants. For the above mentioned methods k equals to 0 (FWO method), 2 (KAS method) and 1.9 to 1.95 for the methods by Starink [26].

From equation (7) we determine the activation energy E and linear fit intercept C which gives frequency factor.

Another method related with isothermal conversion.

When we consider $f(\alpha) = (1-\alpha)^n$, where n is called the reaction order in analogy with homogeneous reactions. When we start from isothermal measurements at different temperatures, we can calculate E_a and A from resulting straight line when using logarithmic form of equation (3).

$$\ln \left(\frac{\left(\frac{d\alpha}{dt} \right) t}{(1-\alpha)^n} \right) = \ln K - \frac{E}{RT} \quad (8)$$

This calculation is repeated for different values of n and the value that gives the highest correlation coefficient is considered to be the best value. The slope and onset give us $-E_a/R$ and $\ln K$, respectively.

For Non-isothermal conversion:

For linear heating rate $\beta = \frac{dT}{dt}$, considered for non isothermal measurements,

The basic equation $\frac{d\alpha}{dt} = Kf(\alpha)\exp - E/(RT)$ can be written as

$$\frac{d\alpha}{dt} = (K/\beta)f(\alpha)\exp - E/(RT),$$

Restricting the function to $f(\alpha) = (1-\alpha)^n$

Taking logarithms on both sides we get

$$\ln\left(\frac{d\alpha}{dT}\right) - \left[n \ln(1-\alpha) - \ln\left(\frac{K}{\beta}\right)\right] - \frac{E}{RT} \quad (9)$$

Kofstad [39] transforms this equation to

$$\ln\left(\frac{[-d\ln(1-\alpha)]}{dt}\right) + (1-n) \ln(1-\alpha) = \ln\left(\frac{K}{\beta}\right) - E_a/RT \quad (10)$$

The value of “n” gives the best correlation coefficient for the resulting straight line is used, and from the slope we can calculate the activation energy E_a .

Ingraham and **Marrier** [10] complicate the formulae by suggesting that the frequency factor A is a linear function of temperature ($A=A' \times T$), but they restrict the value of $n = 0$, zero order reaction, so equation (9) can then be transformed to

$$\log\left(\frac{\beta}{T}\right) \frac{d\alpha}{dT} - \ln A' - \frac{E}{RT} \quad (11)$$

The methods of Kofstad, Ingraham and Marrier give us a value of n ,

These three methods use one single measurement and allow us to calculate E_a from the slope of straight line for a range of value of α .

Here, it should be noted that changing the heating rate and thus the temperature at which the reaction takes place can change the reaction mechanism and thus the activation energy. Therefore methods based on only a single run (one heating rate) are disapproved of by most researchers.

Modulating heating rates

In modulating heating rate methods, a sinusoidal temperature is superimposed on top of a conventional heating profile. This working methods is equivalent to temperature – modulated

DSC, and as a fact, both techniques were devised by Mike reading. The rate of weight loss responds to the temperature oscillations and the use of discrete Fourier transformation allows to calculate the kinetics parameters E_a and A on a continuous basis, making possible the study of the decomposition kinetics as a function of time, temperature and conversion factor, without any assumptions about the reaction mechanism (Model free calculations). The software calculates E_a on the basis of the following equation,

$$E_a = \frac{R(T^2 - A'^2)L}{2A'} \quad (12)$$

Where E_a , R and T have their normal meaning, A' is the temperature amplitude of the applied sinus profile and L for peak and valley differentiation,

2.4.4: Available Literature on Estimation of Activation Energy of blast furnace slag.

The calculation and the meaning of activation energy is always a subject for animated discussions at thermal analysis meeting. All this interested lies in the fact that the value of the activation energy can give an idea about the optimum reaction conditions, thermal stability, and the expected lifetime of a slag to be kept at a certain temperature. So reaction kinetics has always been a point of interest for researcher: as early as 1889 S. Arrhenius won first Nobel Prize in chemistry and in this field many more researchers worked.

Borham, B. M. et al [17] studied the urea nitrate by differential thermal analysis (DTA) curves using the Murray and White equation and various other reaction rate equations and An average activation energy ΔE^\ddagger of 31.7 ± 10.0 kcal/mole was calculated and they have shown that These results illustrate the pronounced effect of self heating on calculation of activation energies. The Kissinger method of calculating the reaction order developed for endothermic DTA peaks produced good results when applied to the present DTA study.

Moynihan, C. T., et al [20]. Studied the activation energy ΔH for structural relaxation in the glass transition region which determined from the heating rate dependence of the glass transition temperature T_g or the cooling rate dependence of the limiting fictive temperature T'_f measured using DSC or DTA.

Keuleers, R. R., J. F. Janssens, et al [23] comparison the effective methods for calculation of activation energy for the thermal decomposition of chemical compounds They have studied for

the comparative study of different measurement and calculation procedures for the thermal decomposition of $\text{Mn(Urea)}_2\text{Cl}_2$.

Starink, M. J, et al studied the Model-free iso-conversion methods which were most reliable methods for the calculation of activation energies of thermally activated reactions and a large number of these isoconversion methods have been proposed in the literature [24]. Type A methods such as Friedman methods make no mathematical approximations, and Type B methods, such as the generalised Kissinger equation [4]. And they found that accuracy of determination of transformation rates is limited, and type B methods will often be more accurate than type A methods.

Homer E. Kissinger et al [18] studied the Variation of Peak Temperature with Heating Rate in Differential Thermal Analysis and found that Changes in heat content of the active sample are indicated by deflections shown by a line representing the differential temperature. It is conventional to represent an endothermic effect by a negative deflection and an exothermic effect by a positive deflection. The deflections, whether positive or negative, are called peaks.

Masashi Nakamoto et al [29] studied the viscosity of molten slag with low melting point to develop an improved blast furnace operation at lower temperature such as 1673 K. They measured the viscosities of molten $\text{CaO-SiO}_2\text{-MgO-Al}_2\text{O}_3$ slag by rotating cylinder method and compared with the results of the model developed. They showed that slag with composition 35% Al_2O_3 -43.1% CaO -7.5% MgO -14.4% SiO_2 has melting temperature below 1673 K and has a viscosity less than 0.6 Pa.s below 1673 K.

Y.S. Lee et al [15] studied the influence of MgO and Al_2O_3 contents on the viscosities of blast furnace slag containing FeO . The viscosities of $\text{CaO-SiO}_2\text{-Al}_2\text{O}_3\text{-MgO-FeO}$ slag were measured under conditions of C/S 1.35-1.45, 10-18% Alumina, 3.5-10% MgO and 5% FeO . They found that on increasing Al_2O_3 content, the viscosity of the slag increased at fixed C/S and MgO content. The viscosity of the slag showed a minimum value at around 7% MgO at temperatures above 1723 K. However, it was not significantly changed with varying MgO content.

Wang, Zhong-jie, et al, [30] studied the crystallization process of glass ceramics prepared from a mixture which was composed of nickel slag, blast furnace slag and a small amount of quartz sand. The crystallization behaviour was studied by differential scanning calorimetry (DSC), X-ray diffraction (XRD) and field emission scanning electron microscope (FESEM). They found shown that the radial crystals were observed when the glass was heated up to

820 °C. By XRD analyzing, the spherical crystals and radial crystals were likely to be the crystals of Diopside ($\text{CaMg}(\text{Si,Al,Fe})_2\text{O}_6$) and Hedenbergite ($\text{CaFe}(\text{Si,Al,Fe})_2\text{O}_6$).

D. Ghosh V.A. Krishnamurthy, et al [31] studied the application of optical basicity to viscosity of high alumina blast furnace slag. In which he found that Experimental measurement of slag viscosity requires high temperature equipment and is time consuming and Viscosity of a slag is strongly influenced by the chemical composition, structure and the temperature and found that The basic oxides namely lime, magnesia, titania are the providers of oxygen, act as network breakers and result in depolymerisation of the melt.

Gan, Lei, et al [9] studied the continuous cooling crystallization kinetics of molten blast furnace slag. Activation Energy obtained is much higher during cooling than that yielded during heating. Result show that akermanite and gehlenite are the major minerals in the continuous cooled crystalline blast furnace slag were investigated by means of X-ray diffraction

Chapter-3

EXPERIMENTAL DETAILS

3. Experimental

3.1. Sample Preparation:

Coning and quartering sampling technique used, which is the reduction in size of a granular or powdered sample, by forming a conical heap which is spread out into a circular, flat cake. The cake is divided radically into quarters and two opposite quarters are combined. The other two quarters are discarded. The process is repeated as many times as necessary to obtain the quantity desired for some final use (e.g. as the laboratory sample or as the test sample). If the process is performed only once, coning and quartering is no more efficient than taking alternate portions and discarding the others. [32]

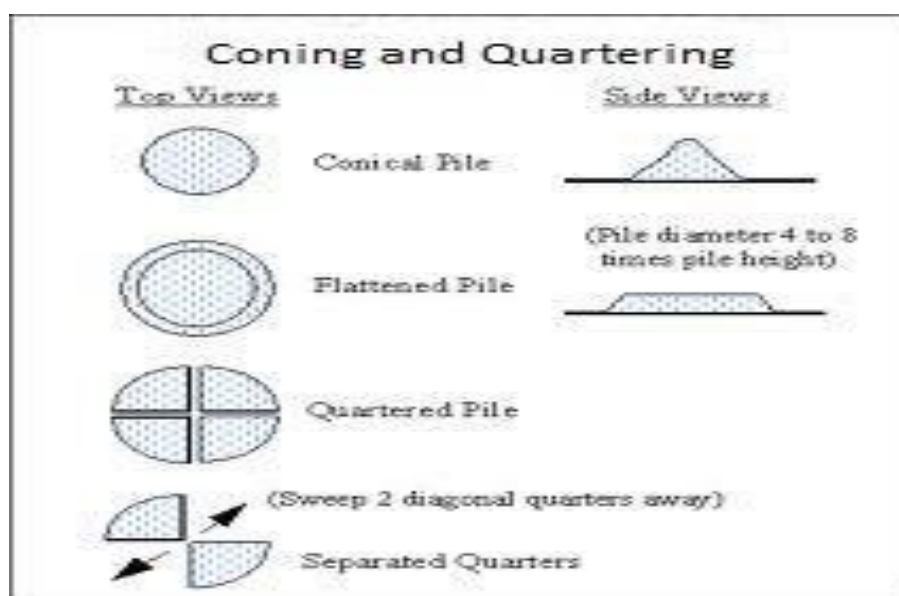


Figure3.1. Coning and Quartering [29]

After Coning and quartering, I did ball milling for forming fine particle size. These mills are also referred as centrifugal mills and are used to grind samples into colloidal Fineness by generating high grinding energy. Here used 300 rpm of revolution and taken 30 minutes for each sample.

For calculation of viscosity, sample preparation start with preheating of sample in air blow furnace which heated sample up to 300°C then it cooled by which it removed moisture and after this it formed fine particle through planetary ball milling.

3.2. Experimental Apparatus

3.2.1 Planetary Ball Mill

These mills are also referred as centrifugal mills and are used to grind samples into colloidal Fineness by generating high grinding energy

This apparatus used for sample preparation to form fine powder of industrial blast furnace slag in the experimental process of DSC. Fig.3.2. Represents a four stationed planetary mill presented by Gilson Company. The samples are placed in one of the vile and numerous balls are added as shown. The vile is covered by the cover plate and then it is mounted in the machine. Once the viles are mounted and secured, the machine is functional. The bowls are independent of the rotatable platform and the direction of rotation of the bowls is opposite to the direction of the rotatable platform. Due to alternate addition and subtraction of the centrifugal forces, the grinding balls rolls halfway in the vile and then thrown across the viles and then impacting the opposite walls at very high speeds. Here used 300 rpm of revolution and taken 30 minutes for each sample.



Figure 3.2- A four station Planetary Ball Mill

3.2.2. Differential scanning calorimetry (TG-DSC).

By using Thermo gravimetric Analyzers STA 409 PC Luxx, Netzsch, Germany, We have studied the thermal analysis of blast furnace slag which gives us peak temperature of phase changed slag.

The Specification of these equipments is,

Sensitivity:	0.001 mg
Mass variation measurement ranges:	± 20 mg, ± 200 mg, ± 2000 mg
Accuracy:	1% of measurement range
Peak load:	18 g
Temperature range:	25 - 1500°C
Rate of temperature change:	0.1 - 50°C/min
Atmosphere:	neutral, oxidative, reducing

In this experimental work we have taken mass of slag sample 20mg, temperature range 25 to 1350°C and rate of temperature change 2,4,6,8,10°C/min.

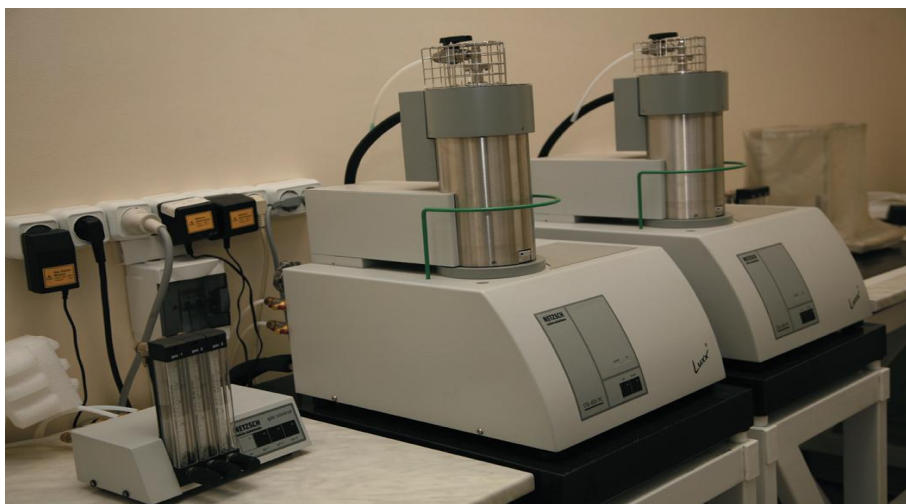


Figure 3.3 Simultaneous Thermo Analysis (TG-DSC or TG-DTA) in wide temperature range

3.2.3. High temperature viscometer

For calculation of viscosity of blast furnace slag we have used High temperature viscometer which is shown in fig. no.3.4, the main purpose of calculation of viscosity is to analyse flow characteristics of liquid slag. And also calculate activation energy of blast furnace slag by viscometer.

This machine has viscosity range 10^1 - 10^8 dPas, Max Temperature 1700°C, crucible material- PtAu5%, max speed-800 rpm, Torque range 0-150mNm, Atmosphere -air or inert ga ,purge gas.

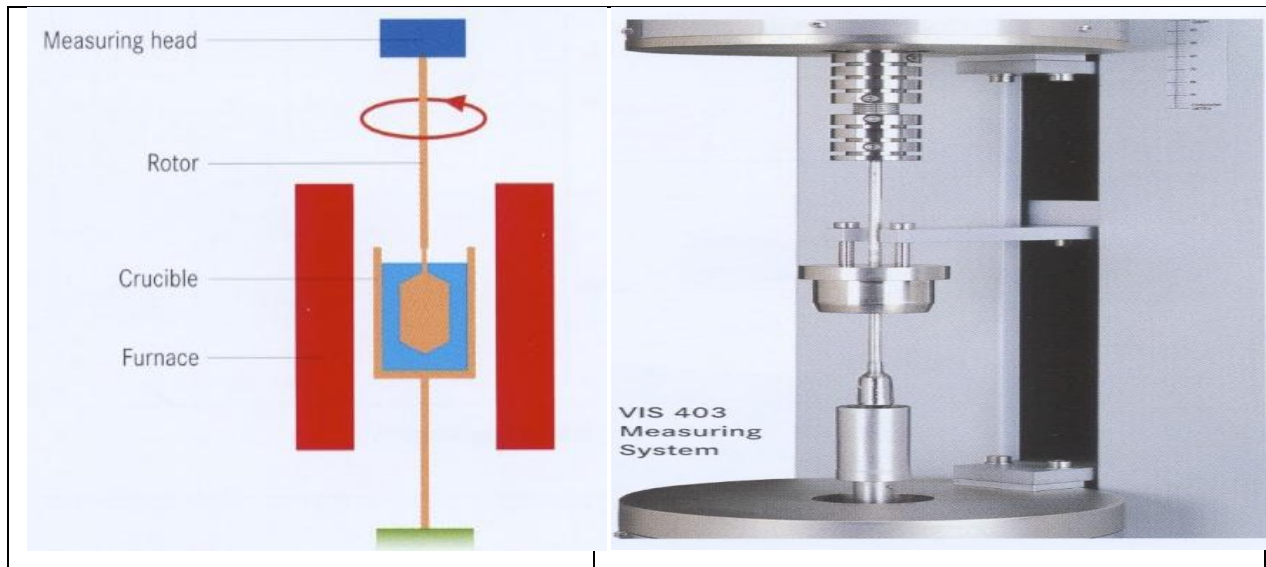


Figure 3.4: VIS 403 Rotating High Temperature Viscometer.

3.2.4. High Temperature Microscope

The Heating Microscope method is adopted for recording the characteristic temperatures. A picture of the Leitz heating microscope is shown in Fig.7. The sample, in the form of a 3 mm cube, is heated in an electric furnace in the microscope assembly. The shape change of the sample as a result of heating is shown by me. A grid-division which is simultaneously observed with the sample and the temperature to which the sample is being heated facilitate identification of the four characteristic temperatures

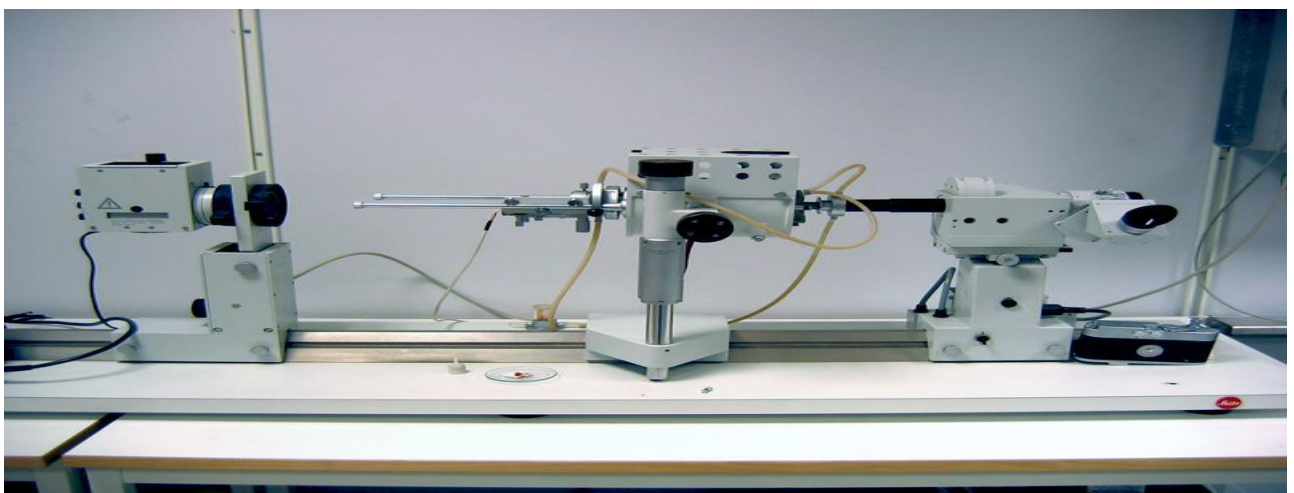


Figure No. 3.5: Pictorial view of Leitz heating microscope

3.2.5. X-ray diffraction (XRD)

X-ray diffraction technique was used to identify the different phases (elemental phase/intermetallic phase/crystalline phase/non-crystalline phase) present in the coating. XRD analysis was done by using Panalytical MPD system. Here Ni- filtered Cu-K α radiation used in X- Ray Diffractometer. d- Values obtained from XRD patterns were compared with the characteristics d-spacing of all possible values from JCPDS cards to obtain the various X-ray peaks. Obtained d-spacing based on the equation;

$$n\lambda = 2d\sin\theta$$

Where, λ = Wavelength of characteristic x-rays., d=Lattice inter-planar spacing of the crystal.& θ = x-ray incident angle.



Figure 3.6: X-ray Diffraction Machine.

3.2.6. Scanning electron microscopic Machine (SEM).

By using JEOL JSM-6480 LV scanning electron microscope (SEM), microstructure of raw power of blast furnace slag before heating and plasma sprayed coated specimens after heating (diffusion) were studied. The surface morphology as well as the coating – substrate interface morphology of all coatings was observed under the microscope. Here SEM mostly using the secondary electron imaging. By the use of this Machine we showed particulates and size of the powder slag sample, and exhibition of melting formation an incongruent mass.



Figure 3.7. Scanning electron microscopic Machine (SEM).

3.3: Experimental Procedure

The experimental procedure is divided in 'Five' parts, the aim being to determine the Activation energy of blast furnace slag and correlate the chemical composition of slag for proposing the flow characteristics that would give slag behaviour with blast furnace. The five part of experimentation include the following,

3.3.1. Collected five Blast Furnace slag from Rourkela steel plant contained different heat.

3.3.2. Determined the chemical composition by adopting the conventional methods. This is given in table no3.1.

Sample	SiO ₂	Al ₂ O ₃	CaO	MgO	TiO ₂	Na ₂ O	K ₂ O	Fe ₂ O ₃	C/S
1	31.86	16.92	38	10.23	0.7	0.98	0.48	0.66	1.192
2	33.25	16.31	36.84	10.56	0.82	1.1	0.52	0.54	1.107
3	32.48	17	35.78	11.88	0.55	1.1	0.52	0.6	1.101
4	31.08	17.04	36.96	11.22	0.5	1.8	0.88	0.40	1.189
5	34.32	16.58	36.2	9.57	0.55	1.36	0.82	0.53	1.054

Table 3.1: Chemical composition (wt.%) of different blast furnace slag.

3.3.3. For Estimation of Activation energy of blast furnace slag we have done two measurements.

A. DSC in which different methods have applied,

- I. Kissinger method.
- II. Ozawa method.

B. Viscosity measurements to examine the validity of the measurement by using DSC.

DSC (Differential Scanning Calorimetry) ANALYSIS

For calculation of Activation Energy of slag DSC analysis has to be done. Firstly we have done sampling of B.F. slag which gave uniformity and fineness of slag sample which is given in section 3.1 and 3.2.1. After sampling of slag we took 20mg of sample for this analysis, this sample placed in the alumina crucible which has also weighted 180mg after this alumina crucible placed in Thermo gravimetric Analyzers STA 409 PC Luxx, Netzsch, Germany. This apparatus shown in 3.2.2;

Before starting of analysis we have done stabilisation of equipment and crucible for 30 min. And then open correction file of machine to finding out correction factor for different heating rate (2, 4, 6, 8, 10⁰C/min.) of the sample.

The DSC furnace temperature is controlled by a cam-driven program controller. A current interrupter in the cam motor circuit allows any heating rate up to about 25⁰C/min.

The differential scanning is measured between the centres of the active and reference sample. The reference sample is α -aluminium oxide. The DSC and Temperature are recorded on the same chart by a multipoint recorder. A typical pattern of sample has shown in figure no 9, 10, 11, and 12.

Each of the five sample materials were run in DSC in the alumina crucible holder at about heating rate 2, 4, 6, 8, 10⁰C/min. After finding the DSC curve of sample we have applied two methods for calculation of Activation Energy which have derived from **Arrhenius** equation is

- I. Kissinger method.
- II. Ozawa method.

Calculation based on Kissinger equation was-

$$\ln (\phi/T_p^2) = -E_a/RT_p + \text{Constant.}$$

Where ϕ is heating rate in K/min.

T_p is peak point temperature in (k) at melting point of slag,

R is universal Gas constant = 8.314 J/mol-k,

E_a is Activation Energy in KJ/mole

Now Graph plotted between $\ln (\phi/T_p^2)$ in Y axis, and $1/T_p$ in X axis and we obtained slope which is equal to $-E_a/R$, from this we get Activation energy E_a (KJ/mole).

Calculation based on Ozawa equation –

$$\ln(\phi) = -E_a/T_p R + \text{constant.}$$

Where ϕ is heating rate in K/min. T_p is peak point temperature in (k), R is universal Gas constant = 8.314 J/mol-k, E_a is Activation Energy in KJ/mole.

Now Graph plotted between $\ln (\phi)$ in Y axis, and $1/T_p$ in X axis and we obtained slope which is equal to $-E_a/R$, from this we get Activation energy E_a (KJ/mole).

VISCOSITY ANALYSIS

Viscosity involves transporting one layer of liquids over another layer i.e. flow phenomena. The mobility of ionic species present in the slag determines its viscosity.

Experimental procedure for calculation of viscosity of slag starts with sampling, for this Sample No 3 (C/S=1.101) was prepared as fine particle, then sample placed in platinum crucible and then this crucible placed in furnace where it heated up to 1400°C for complete melting and after it cooled in open atmosphere. Then it was found that it reduced by volume with 60% of the crucible after it was ready for placement in viscosity measurement instrument.

This analysis part consists of the VIS 403 Rotating High Temperature Viscometer which has shown in 3.2.3, the fused power slag which was in platinum crucible placed in furnace chamber of viscometer which is attached with thermocouple gives reading of heating temperature. All

these equipments were connected with computer programmer. The sample material was run with heating, holding and cooling temperature. All this time and Temperature of slag sample were given in the computer programmer.

We have given heating range up to 1000⁰C then holding for 5 min. And again heating up to 1400⁰C. After heating we got the slag fully converted in liquid form so after this stage rotor of this instrument rotated manually for free rotational test and then operating system gives a command for cooling and slow down the position of rotor which goes downward with slow motion and then rotor rotate at the speed 100rpm. After this experiment we obtain viscosity of slag during cooling with cooling rate 5⁰C/min.

The calculation of viscosity by this instrument based on Arrhenius equation [16] mainly depends on temperature and chemical composition.

$$\dot{\eta} = A \cdot \exp (E/RT).$$

Where $\dot{\eta}$ is viscosity of slag during cooling (d pas), E is Activation Energy , R is universal Gas constant =8.314 J/mole, T is Temperature in Kelvin

3.3.4 HEATING MICROSCOPE ANALYSIS

Flow characteristics measurements of the sample are carried out by this experiment. Specially this experiment is carried out to have a chance of the Tp (melting point) as defined from DSC and from HT (hemispherical temperature). Sampling for heating microscope is the same procedure as DSC sampling has taken.

Analysis part consists of the high temperature microscopy shown in figure no- (Leitz heating microscope) was used for flow characteristics temperature measurement. The powdered slag is prepared in the form of small cubic shapes for this measurement. They are mounted in the heating microscope. The sample gets heated gradually and deformation takes place. This deformation defines the flow characteristics of the slag in the form of IDT (initial deformation temperature), ST (softening temperature), HT (hemispherical temperature) and FT (fusion temperature). There is a control of heating rate, water is used as coolant and there is a camera attached to take photographs of different characteristics temperature of slag when required.

3.3.5 XRD ANALYSIS

Phase Analysis of sample was carried out by using X-pert MPD system (PAN Analytical) X-ray Diffraction Techniques (XRD). Which is shown in figure no-8.

Sample for this instrument were taken same as DSC analysis. In XRD analysis both powder sample and fused powder sample were taken and this was placed in sample holder of XRD machine where it was operated in scanning range $10-90^{\circ}(\theta)$ and step speed $3^{\circ}\text{C}/\text{min}$. Here Ni-filtered $\text{Cu-K}\alpha$ radiation used in X-Ray Diffractometer. This range of XRD applied for all five samples for getting Phase analysis.

3.3.6 SEM ANALYSIS

SEM were carried out to understand fusion behaviour of the slag sample, this is carried out by SEM (JEOL-JSM840) machine. This has been shown in figure no 9.

Prior to Microscopy analysis the fused samples were mounted on a metal stub with carbon paint. In a vacuum evaporator the samples were thin coated with palladium-gold under vacuum of 0.01 torr to make the surface conducting for viewing through SEM. The mounted specimens were studied by SEM (JEOL-JSM840).

Microstructures of the sintered specimens were analyzed using a scanning electron microscope. The system set up is shown in the fig. No... Scanning electron microscope was used to study the micro structural feature of samples as it has a much greater resolution power compared to the optical microscope. In SEM, a hot tungsten filament electron gun, under vacuum emits electrons; which pass through a series of electromagnetic lenses. The sample is then bombarded with a fine beam of electrons. The acceleration potential ranges from 1-30 KV. A part of the beam is reflected back as back-scattered electrons. The electron beam produced by tungsten filament is of $50\mu\text{m}$ in diameter. Images formed from the secondary electron beam were studied in the extrinsic mode of SEM. While the images obtained appear very real and as if they were photographed by ordinary means, the apparent illumination is a function of particle emission. These particles emitted are termed secondary electrons, and their detection via detector is displayed on a scanning TV display. A bright image will be the result of high secondary electron emission, while the primary influence on high emission is the surface structure of the specimen. The end result is therefore brightness associated with surface characteristics and an image that looks very much like a normally illuminated subject.

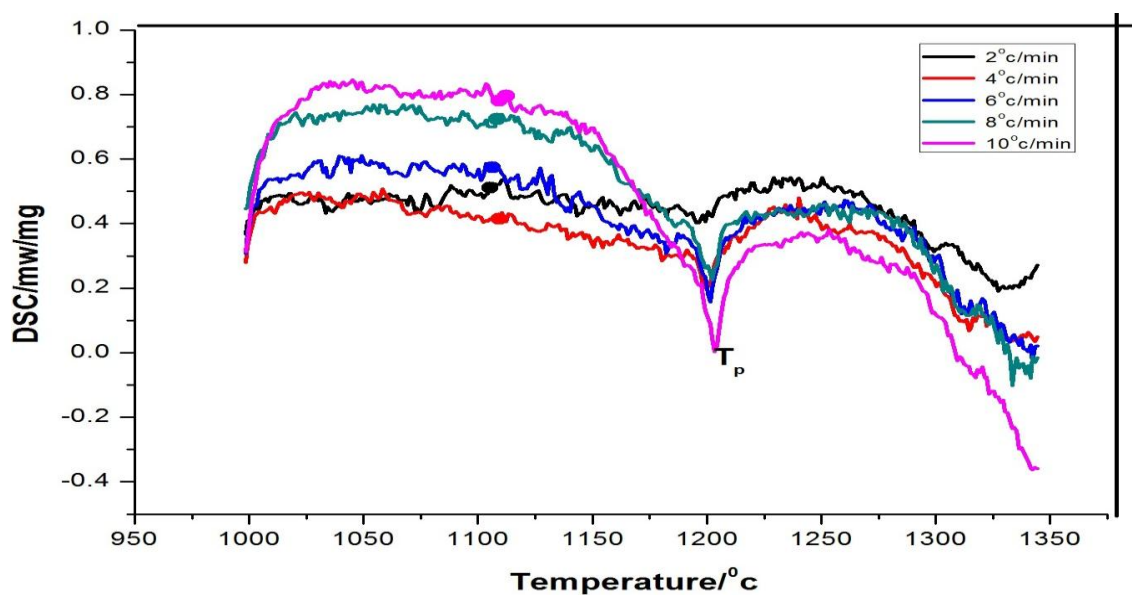
Chapter-4

RESULTS AND DISCUSSION

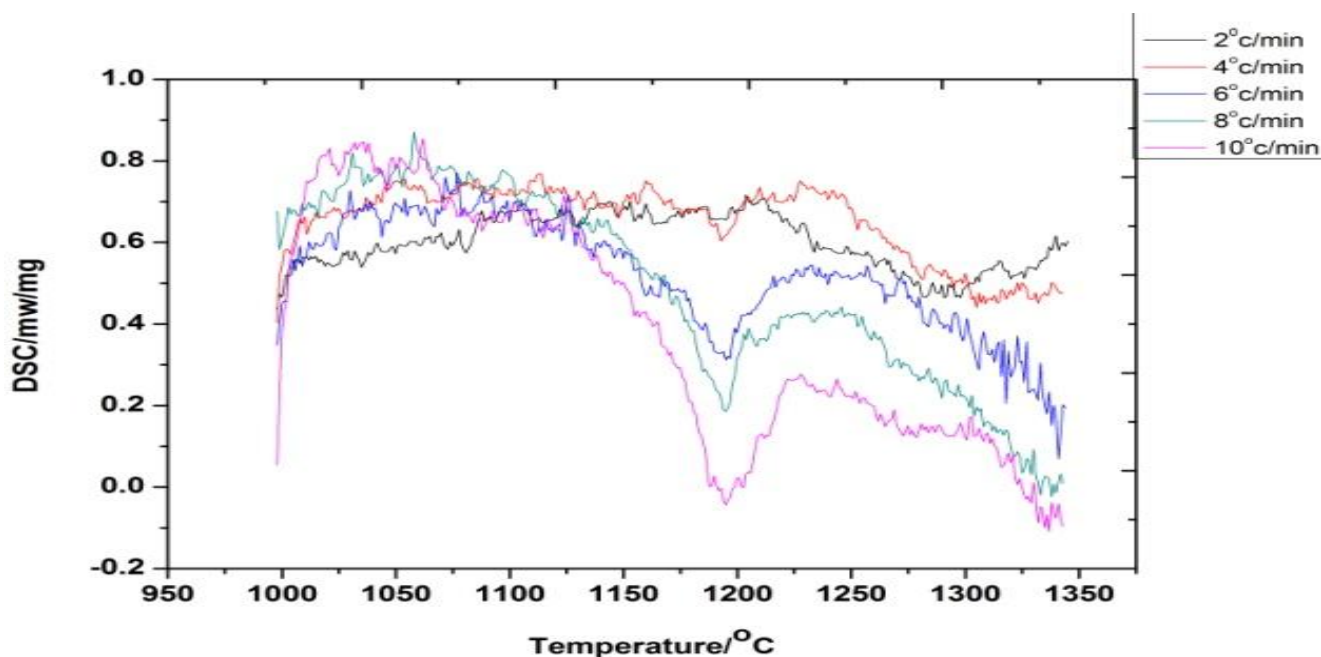
4.1 Results

4.1.1 Activation energy calculation

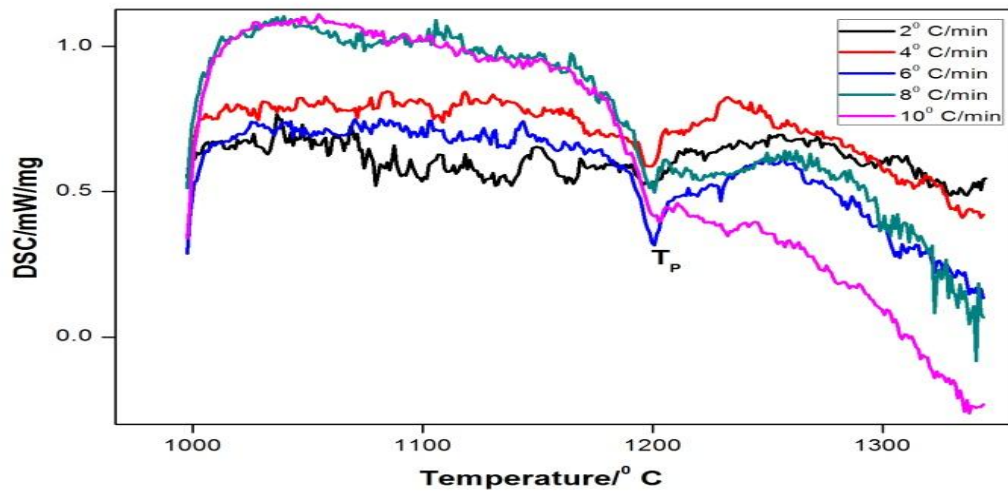
Thermal analysis of blast furnace slag is carried out by DSC (Differential Scanning Calorimeter) measurement to determine the crystallization mechanism as mentioned in Section (2.4.3). Figure 4.1-shows four DSC curves of finely powdered blast furnace slag sample whose C/S ratio 1.192., 1.107, 1.101, and 1.189 respectively.



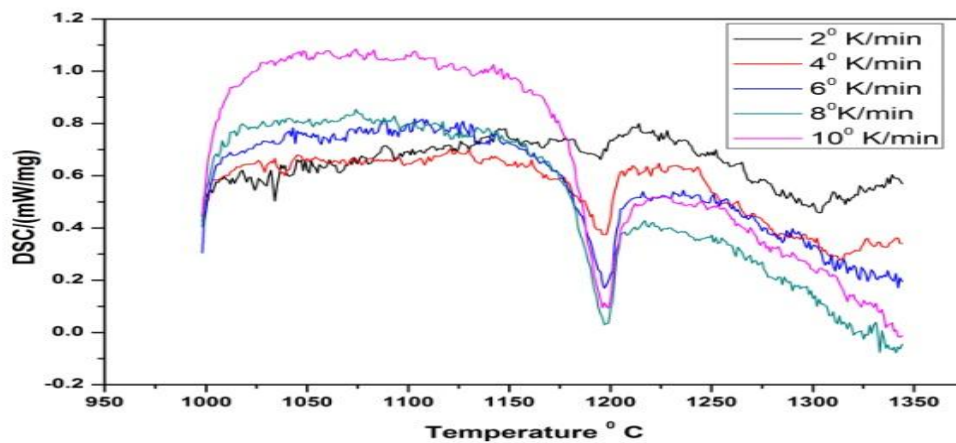
(b)



(c)



(c)



(d)

Figure 4.1 DSC curves of four powdered slag samples: (a) sample 1, (b) sample 2, (c) sample 3 and (d) sample 4. At different heating rates (@ 2, 4, 6, 8, and 10 °C/min.).

Calculation of Activation Energy by DSC is based on two different methods which have derived from **Arrhenius** equation this is

1. Kissinger method: - $\ln(\phi/T_p^2) = -E_a/RT_p + \text{Constant}$

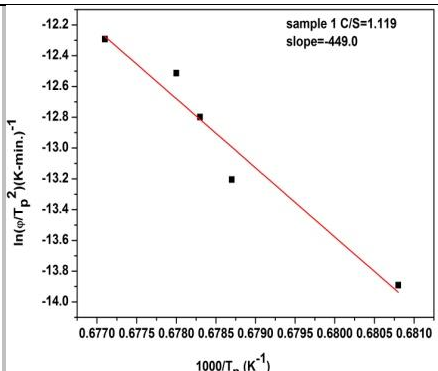
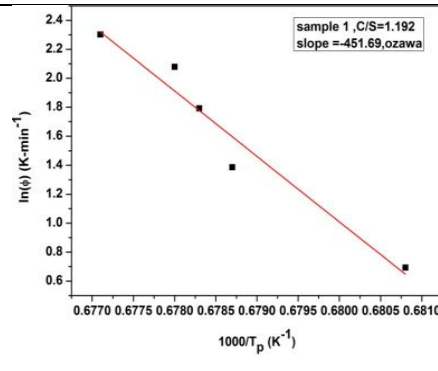
2. Ozawa method: - $\ln(\phi) = -E_a/T_p R + \text{constant.}$

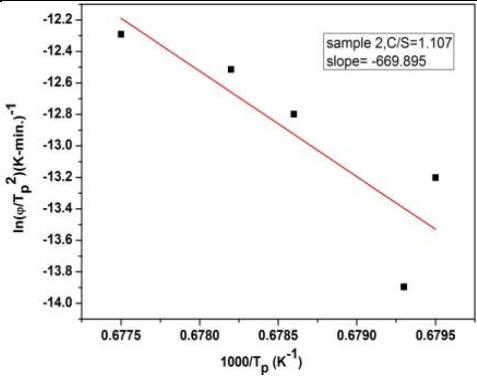
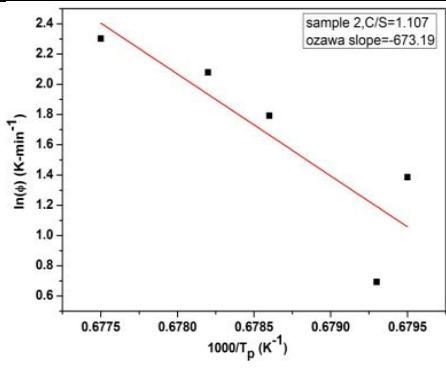
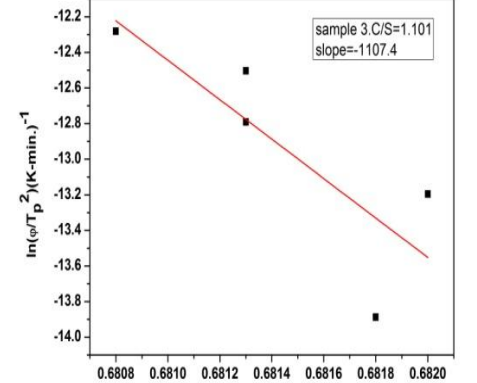
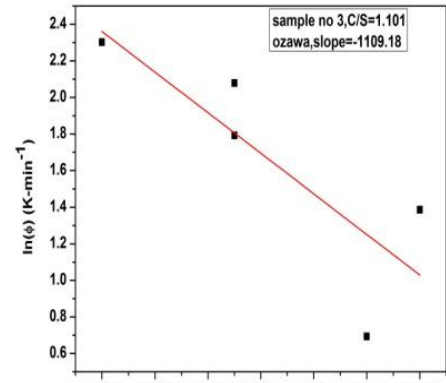
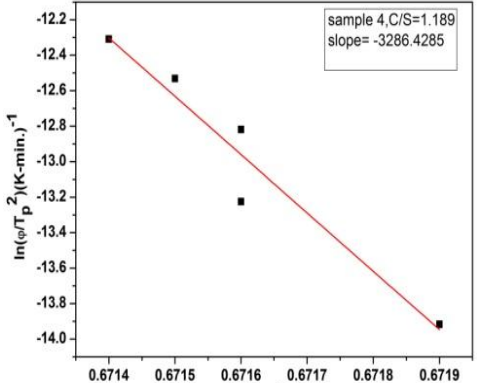
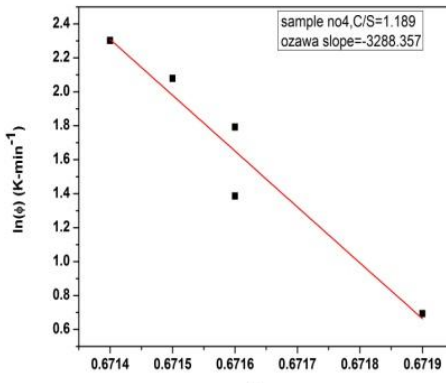
Calculation of Peak Temperature from DSC curve of different sample. At different heating rate. The glass-transition temperature, T_g , was determined as the point of intersection of the straight-lines extending from the tangents of the DSC curves in the region of the baseline shift. Some similar features of each thermo gram are apparent: (a) a reversible endothermic peak at beginning of crystallization temperature, corresponding to the glass-transition temperature, T_g ; (b) exothermic events with maxima in the range of 1000 to 1100°C, indicating crystallization, T_c ; (c) endothermic events at about 1280±1315°C, involving the melting of some crystal phases, T_p (K).

$\phi(^{\circ}\text{C}/\text{min})$ Heating rate	$W_o(\text{mg})$	$T(\text{min.})$	$T_p(\text{k})$ sample 1 $C/S=1.192$	$T_p(\text{k})$ sample 2 $C/S=1.107$	$T_p(\text{k})$ Sample 3 $C/S=1.101$	$T_p(\text{k})$ Sample 4 $C/S=1.18$
2	25.00	287	1468.8 K	1472.1 K	1466.6 K	1466.6K
4	25.00	199.5	1473.2 K	1471.6 K	1466.2 K	1469.2K
6	25.00	170.3	1474.2 K	1473.5 K	1467.7 K	1469.5K
8	25.00	155.75	1474.8 K	1474.4 K	1467.6 K	1471.3K
10	25.00	147	1476.8 K	1476 K	1468.7 K	1471.2K

Table 4.1: Peak temperature of different obtained from DSC curve.

Table 4.2: Estimation of A.E. using, (a) Kissinger & (b) Ozawa method for different blast furnace slag.

Sample No. and C/S ratio	Kissinger method	Ozawa method
Sample 1, $C/S=1.192$	 <p>A.E= 3732.50 KJ/mole.</p>	 <p>A.E = 3755.35 KJ/mole.</p>

sample 2 C/S=1.107	 <p>sample 2, C/S=1.107 slope=-669.895</p> <p>A.E = 5569.50 KJ/mole</p>	 <p>sample 2, C/S=1.107 ozawa slope=-673.19</p> <p>A.E = 5596.90 KJ/mole</p>
sample 3 C/S=1.101	 <p>sample 3, C/S=1.101 slope=-1107.4</p> <p>A.E = 9202.43 KJ/mole</p>	 <p>sample no 3, C/S=1.101 ozawa slope=-1109.18</p> <p>A.E = 9221.72 KJ/mole</p>
sample 4 C/S=1.189	 <p>sample 4, C/S=1.189 slope=-3286.4285</p> <p>A.E = 5758.52 KJ/mole</p>	 <p>sample no4, C/S=1.189 ozawa slope=-3288.357</p> <p>A.E = 5815.31 KJ/mole</p>

The activation energy for crystallization is an important kinetic parameter for the determination of thermal stability of the amorphous phase. Based on the results of the exothermic peak shift in DSC measurements conducted at different heating rates, the value of activation energy was calculated using Kissinger [18] and Ozawa [33] equations.

The dependence of crystallization temperature on heating rate was used to determine the associated activation energy by means of Kissinger equation $\ln(\dot{\Phi}/T_p^2) = -E_{ac}/RT_p + \text{constant}$ and Ozawa equation $\ln \dot{\Phi} = -E_{ac}/T_p + \text{constant}$

Where $\dot{\Phi}$ is the heating rate, T_p is the peak temperature in DSC scans, R is gas constant having value $8.3145 \text{ J.mol}^{-1}.\text{K}^{-1}$ with slope $-E_{ac}/R=B$, where B is a constant.

Data on heating rate and peak temperature was plotted in terms of $1000/T_p$ vs $\ln(\dot{\Phi}/T_p^2)$ for Kissinger equation and $1000/T_p$ vs $\ln \dot{\Phi}$ for Ozawa equation, as shown in table no 4, respectively. The linear fit of the data resulted in slope, $(A.E)/R = B$. The value of the slope B was measured from the plots. Putting the values of R and B , activation energies for the first stage crystallization by Kissinger and Ozawa methods designated as $(A.E-K)$ and $(A.E-O)$ were calculated and the results are summarized in Table 4.2.

Relation of Activation Energy vs. C/S value of slag:

From the given tabulation value and plot between Activation Energy vs. C/s ratio gives the conclusion that As the C/S ratio increases the Activation Energy values decreases and so viscosity of slag decreases.

Due to increase of c/s value basic oxide namely lime, magnesia provide oxygen, act as network breakers and result in depolymerisation of the melt there by decreasing the viscosity .

C/S value of slag	A.E by Kissinger methods Kj/mole	A.E by Ozawa methods Kj/mole
1.101	9202.43	9221.72
1.107	5569.50	5596.90
1.189	5758.52	5815.31
1.192	3732.50	3755.35

Table 4.3.Tabulation of Activation Energy and C/s ratio by different methods

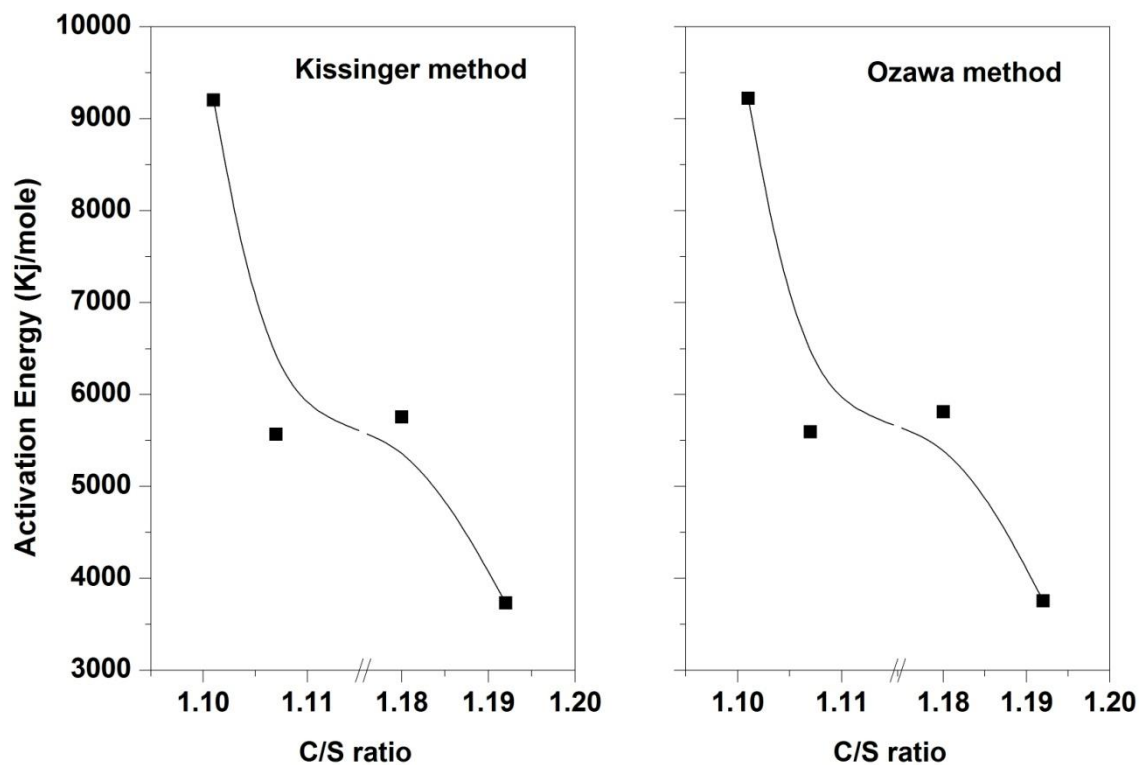


Figure 4.2: Activation Energy vs. C/S ratio plot.

From this plot we found that as the C/S ratio of slag increases Activation Energy decreases. So also viscosity of slag decreases and hence flow characteristics of increases.

Relation between Activation Energy and MgO% value of slag

Here we have given table which give the relation between Activation Energy and MgO% as calculated by Kissinger and Ozawa methods

MgO%	A.E by Kissinger methods Kj/mole	A.E by Ozawa methods Kj/mole
10.23	3732.50	3755.35
10.56	5569.50	5596.90
11.22	5758.52	5815.31
11.88	9202.43	9221.72

Table 4.4: Tabulation of Activation Energy and MgO% by different method

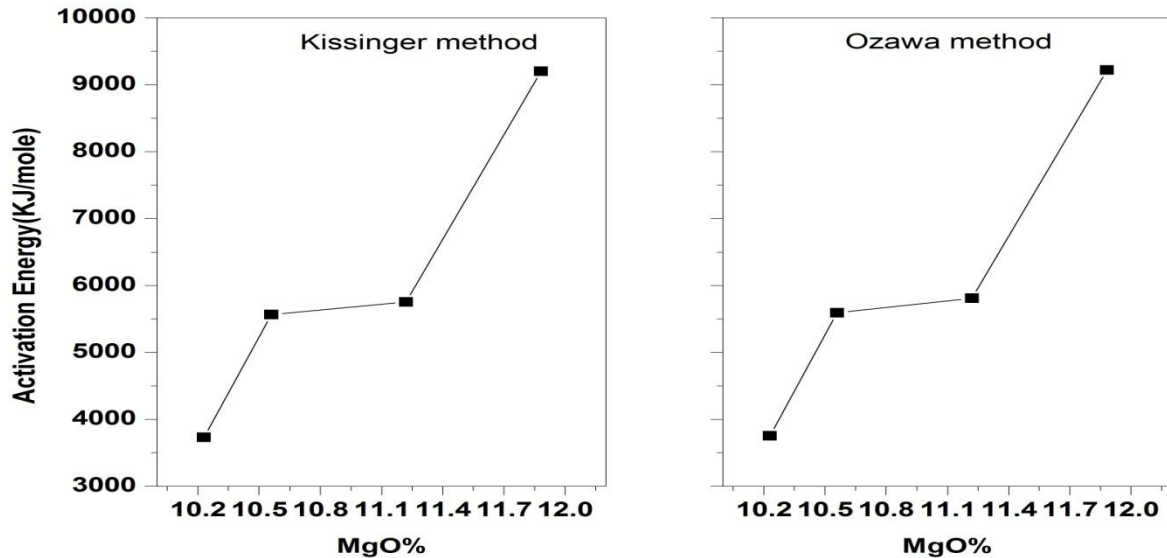


Figure 4.3: Plot between Activation Energy vs. MgO%

This plot also shows that as the MgO% increases Activation Energy increases up to 10.56% of MgO contain and then it does not show any significant variation till 11.2% MgO. Beyond 11.22% MgO the Activation Energy again shows an abrupt increase with increase of MgO percentage.

4.1.2 VISCOSITY MEASUREMENTS

In our experimental work calculation of viscosity of blast furnace slag is done by VIS 403 Rotating High Temperature Viscometer which has viscosity range 10^1 - 10^8 dPas, Max Temperature 1700°C ,

In viscosity measurement rate of cooling from liquid phase has adopted $5^\circ\text{C}/\text{min}$.

The calculation of viscosity by Arrhenius equation [16] mainly depends on temperature and chemical composition.

$$\dot{\eta} = A \cdot \exp(E/RT).$$

Where $\dot{\eta}$ is viscosity of slag during cooling (d pas), E is Activation Energy , R is universal Gas constant = 8.314 J/mole , T is Temperature in Kelvin .

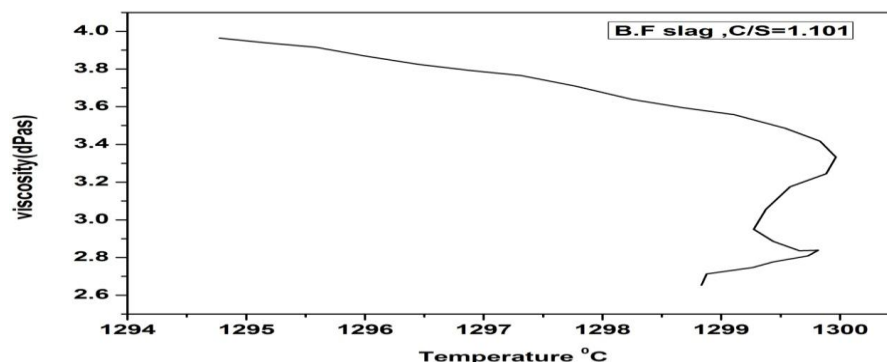


Figure 4.4. Viscosity vs. Temperature graph.

The calculation of viscosity of blast furnace slag has done by the Arrhenius equation. From the given plot of viscosity we obtained viscosity 2.95 dPas at 1299.3°C of slag sample 3. Which chemical composition is given in table no 1.

From this value we have calculated logarithmic value of slag viscosity and this gives the Activation Energy 3906.1002 KJ/mole. Which is approximately same value is as obtained from DSC analysis.

4.1.3 XRD ANALYSIS

Phase analysis is carried out by using X-ray Diffraction pattern.

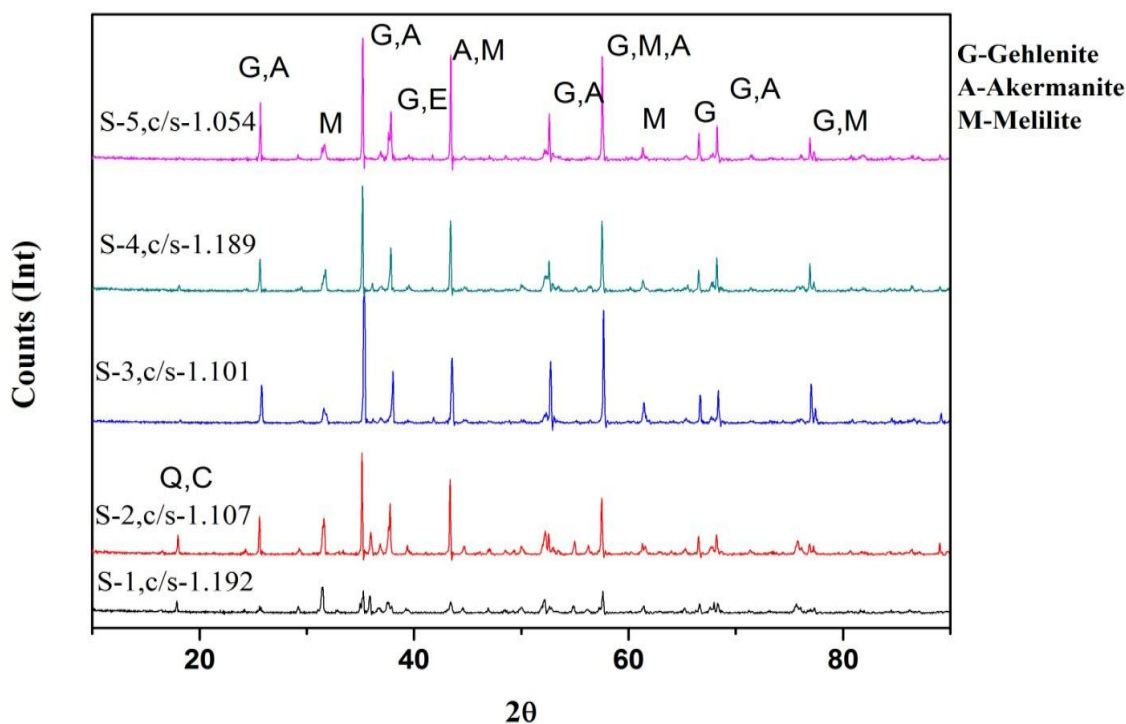


Figure 4.5 XRD pattern of slag sample.

Phase analysis of diffused Blast Furnace Slag gives Idea about change of chemical composition during crystallization temperature which is given in fig no 14. Where G is Gehlenite ($\text{Ca}_2\text{Al}_2\text{SiO}_7$), A is Akermanite ($\text{Ca}_2\text{MgSiO}_7$), and M is Melilite ($(\text{Ca},\text{Na})_2(\text{Al},\text{Mg},\text{Fe})(\text{Si},\text{Al})_2\text{O}_7$) is major constituents

4.1.4 Flow characterisation of blast furnace slag.

The flow characteristics of 5 blast furnace slag samples were measured using the **High Temperature Microscope**. The flow characteristics give four characteristics temperature, viz. Initial Deformation Temperature (IDT), Softening Temperature (ST), Hemispherical Temperature (HT) and Flow Temperature (FT). The flow characteristics of the sample no 1 is represented in fig no 15.

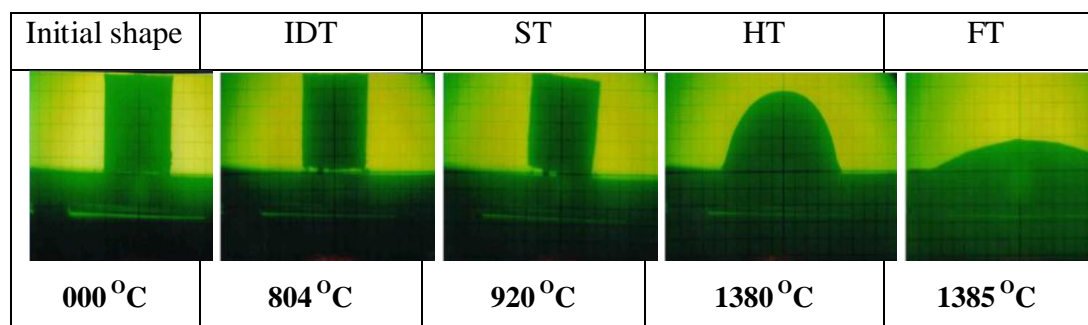


Figure 4.6: flow characteristic image of sample.

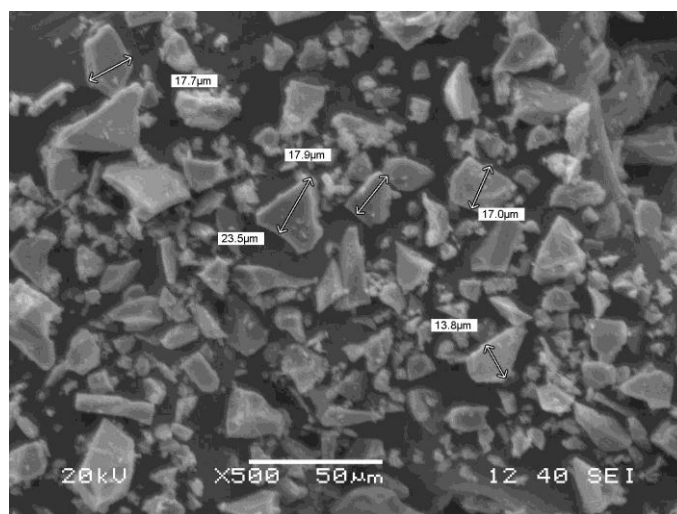
The flow characteristics of 5 blast furnace slag samples measured by High Temperature Microscope have the same value of Hemispherical Temperature (HT). As obtained by the DSC value of slag melting temperature T_p .

Sampe no.	CaO %	SiO ₂ %	MgO %	Al ₂ O ₃ %	C/S	IDT ^o C	ST ^o C	HT ^o C	FT °C	FT-ST °C
1	38	31.86	10.23	16.92	1.192	804	920	1380	1385	465
2	36.84	33.25	10.56	16.31	1.107	816	910	1378	1384.8	474.8
3	35.78	32.48	11.88	17	1.101	810	894	1379	1390	496
4	36.96	31.08	11.22	17.04	1.189	800	889	1370	1386	497
5	36.2	34.32	9.57	16.58	1.054	795	870	1374	1382	512

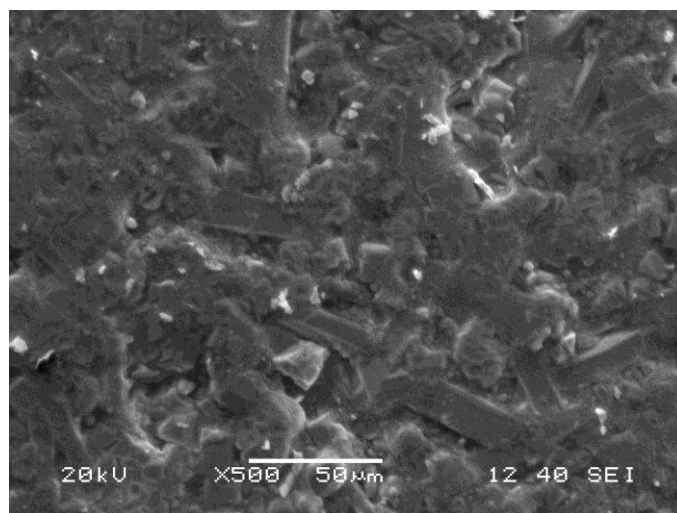
Table 4.5: Composition and flow characteristics of blast furnace slag sample obtained.

4.1.5 Microstructure:

Fig. 4.7(a) shows the scanning electron microscopic images of the powder blast furnace sample and Fig.4.7 (b) shows the scanning electron image of diffused blast furnace slag sample from this image we have observed particulate and size of slag sample before diffusion and after diffusion which gave average value of powder slag sample was 22 micrometer. And we have also shown the exhibition of melting forming an incongruent mass. This is shown in figure 4.7 (a) and (b).



(a)



(b)

Figure 4.7(a) SEM micrographs at 500 magnifications of powder sample, (b) SEM micrographs at 500 magnification of sample no 1 whose C/S ratio is 1.192.

4.2 Discussion

The Activation Energy values obtained in the present case are found to be very high. This is true when any of the two equations are used. Similar observations are reported by Lei Gan, Lei, et al [9]. Which reports the Activation Energy of crystallization of Blast Furnace Slag, They got a value of 1021-1969 KJ/mol, as against 457.5 KJ/mol for B.F. slag as reported by Francis et al [34]. And 125.4-627 KJ/mol for CaO-MgO-Al₂O₃-SiO₃ slag as reported by J. Williamson et al [35]. The obtained high value are attributed to the difference of crystallization mechanism as adopted by the different phases identified in the XRD plot & similar reasons may hold for the present case. For example if we consider the XRD plot for slag no 3. We find the major constituents phases are Gehlenite, Akermanite and Melilite [36]. All the phases have tetrahedral unit cells. But the volume of the unit cells is different. While Gehlenite unit cell has a volume of 300.3[A°]³, Akermanite unit cell has volume of 307.22[A°]³, and Melilite 303.27[A°]³, the basic unit cell which also is tetrahedral, has a volume of 173.39[A°]³ [37]. The above explains that the formation of the different unit cells of different phases by the presence of different constituents lime CaO, MgO etc. In to the silicate tetrahedral network while breaking the silicate network which accounts for the lower value of the Activation Energy of viscous flow, might have also been responsible for the rise of the Activation energy by consisting a stress in the silicate unit cell [38, 39].

The activation energy calculated by viscometer has the approximate same as the DSC activation energy of sample 3. and we get variation of activation energy with the change the value of C/S ratio. This is due to increase of c/s value basic oxide namely lime, magnesia provide oxygen, act as network breakers and result in depolymerisation of the melt there by decreasing the viscosity of the slag so also decreasing the activation energy of slag [40]. In this present work we observed that as the MgO% increases Activation Energy increases up to 10.56% of MgO contain and then it does not show any significant variation till 11.2% MgO. Beyond 11.22% MgO the Activation Energy again shows an abrupt increase with increase of MgO percentage.

Chapter-5

CONCLUSION

5. Conclusions

1. Methods adopted for the calculation of activation energy gave identical values by DSC analysis.
2. The values of activation energy obtained by DSC analysis also matched with the results of viscosity measurement.
3. As the C/S ratio increases the Activation Energy decreases.
4. As the MgO percentage increases the Activation Energy increases up to 10.56% of MgO and then after 11.22% of MgO abruptly increases Activation Energy.
5. The calculated value of Activation Energy was much higher may be due to lattice strain in the silicate structure.

FUTURE SCOPE

The study may be continued for more number of blast furnace slag with variation of C/S ratio and MgO%, to estimate and correlate activation energy of blast furnace slag. Estimation of activation energy by viscosity measurement has not been completed in the present study; this may be characterized extensively. It also required to estimate activation energy of pure oxides to understand the large values of activation energy (as predicted in the present study). Also activation energy of crystallization and viscous flow may be examined to understand such large values of activation energy.

REFERENCE

1. Book: Gupta S. S., and Chatterjee A., "Blast Furnace Iron Making", SBA Publication
2. Behera R. C., Mohanty U. K., and Mohanty A. K., High Temperature Materials and Processes, 9, 1990, pp. 57-75
3. Book: O.P.Khanna "material science and metallurgical ", dhanpat rai publications
4. H.E. Kissinger, J. Res. Nat. Bur. Stand. 57 (1956) 217
5. Zhang, Lunyong, Dawei Xing, and Jianfei Sun. "Calculating activation energy of amorphous phase with the Lambert W function." *Journal of thermal analysis and calorimetry* 100.1 (2010): 3-10.
6. Keuleers, R. R., J. F. Janssens, and H. O. Desseyn. "Comparison of some methods for activation energy determination of thermal decomposition reactions by thermogravimetry." *Thermochimica acta* 385.1 (2002): 127-142.
7. Nippon Slag Association conducts investigations, research, and promotion related to iron and steel slag products
8. Ozawa T (1971) Kinetic of non-isothermal crystallization. *Polymer* 12:150–158
9. Gan, Lei, et al. "Continuous cooling crystallization kinetics of a molten blast furnace slag." *Journal of Non-Crystalline Solids* 358.1 (2012): 20-24.
10. German Industrial Standard 51730
11. JEGEL. Steel Slag Aggregates *Use in Hot Mix Asphalt Concrete*. Final Report, prepared by John Emery Geotechnical Engineering Limited for the Steelmaking Slag Technical Committee, April, 1993.
12. Muller J. And Erwee M., Southern African Pyrometallurgy, 2011
13. Shankar Amitabh, Gernerup Marten, Lahiri A.K, Seetharaman S., Experimental Investigation of the Viscosities in CaO-SiO₂-MgO-Al₂O₃ and CaO-SiO₂-MgO-Al₂O₃-TiO₂ Slags, *Metallurgical and Materials Transactions B*, 38 (6), pp. 911-915
14. Jose M franco and pedro partal. Campus de "El karmen". 21071. Huelva spain,
15. Y.S.Lee, J.R.Kim, S.H.Yi and D.J.Min; "viscous behavior of CaO- SiO₂- Al₂O₃-MgO-FeO slag". Proceedings of VIII international conference on molten slag, fluxes and salts, The South African Institute of Mining and Metallurgy, 2004, p.225.
16. Bottinga, Yan, and Daniel F. Weill. "The viscosity of magmatic silicate liquids; a model calculation." *American Journal of Science* 272.5 (1972): 438-475.
17. Borham, B. M., and F. A. Olson. "Estimation of activation energies from differential thermal analysis curves." *Thermochimica Acta* 6.4 (1973): 345-351.

18. Kissinger, Homer E. "Reaction kinetics in differential thermal analysis." *Analytical chemistry* 29.11 (1957): 1702-1706.
19. Mohanty U.K., Thermo physical properties of some metallothermic slags, Ph.D. Dissertation, R.E. College, Rourkela, 1998
20. Moynihan, C. T., et al. "Estimation of activation energies for structural relaxation and viscous flow from DTA and DSC experiments." *Thermochimica acta* 280 (1996): 153-162.
21. Mittemeijer EJ (1992) *J Mater Sci* 27:397
22. Ozawa T (1970) *J Therm Anal* 2:301
23. Biswas A.K., Principles of Blast Furnace Ironmaking, Calcutta: SBA Publications, 1984
24. Ghosh Ahindra and Chatterjee Amit, Ironmaking and Steelmaking – Theory and Practice, New Delhi: PHI Learning Private Limited
25. Starink MJ (2003) *Thermochim Acta* 404:163
26. Starink, M. J. "Activation energy determination for linear heating experiments: deviations due to neglecting the low temperature end of the temperature integral." *Journal of materials science* 42.2 (2007): 483-489.
27. P. Kofstad, *nature* 179(1957),1362.
28. Gan, Lei, et al. "Continuous cooling crystallization kinetics of a molten blast furnace slag." *Journal of Non-Crystalline Solids* 358.1 (2012): 20-24.
29. Nakamoto Masashi, Tanaka Toshihiro, Lee Joonho and Usui Tateo, *ISIJ International*, Vol. 44, No. 12, 2004, pp. 2115-2119
30. Wang, Zhong-jie, et al. "Crystallization behavior of glass ceramics prepared from the mixture of nickel slag, blast furnace slag and quartz sand." *Journal of Non-Crystalline Solids* 356.31 (2010): 1554-1558.
31. D. Ghosh, V.A. Krishnamurthy and S.R. Sankaranarayanan, *J. Min. Metall. Sect. B-Metall.* 46 (1) B (2010) 41 – 49
32. National Slag Association. *Practical data on use of mineral aggregates: tables, tests, facts and figures*. National Slag Association, 1949.
33. Ozawa T (1970) *J Therm Anal* 2:301
34. A.A. Francis, *J.Am.Ceram.Soc.* 88 (2005) 1859.
35. J.Williamson, A.J.Tioole, P.S.Rogers, *J.Iron Steel Inst.* 206(1968) 898.
36. H.R. Wang, Y.L. Gao, Y.F. Ye, G.H. Min, Y. Chen and X.Y. Teng: *J. Alloy. Compd.*, 2003, **353**, 200. Microstructural Studies Group, Physics Division, Pakistan Institute of Nuclear Science and Technology (PINSTECH), P.O. Nilore, Islamabad, Pakistan.

[http://dx.doi.org/10.1016/S1005-0302\(11\)60104-7](http://dx.doi.org/10.1016/S1005-0302(11)60104-7)

37. Hou, Jungang, et al. "Peroxide-based route assisted with inverse microemulsion process to well-dispersed Bi₄Ti₃O₁₂ nanocrystals." *Journal of Nanoparticle Research* 12.5 (2010): 1797-1805.
38. IUPAC Compendium of Chemical Terminology, 2nd Edition, 1997
39. Soliman A. Derivation of the Kissinger equation for non-isothermal glass transition peaks. *J Therm Anal Cal.* 2007;89(2):389–92.
40. Keuleers, R. R., J. F. Janssens, and H. O. Desseyn. "Comparison of some methods for activation energy determination of thermal decomposition reactions by thermogravimetry." *Thermochimica acta* 385.1 (2002): 127-142.